Physics – Uspekhi **38** (8) 845 – 875 (1995) ©1995 Jointly Uspekhi Fizicheskikh Nauk and Turpion Ltd

PACS numbers: 61.72.Lk; 71.55.Cn; 72.80.Cw

Charged dislocations in semiconductor crystals

V B Shikin, Yu V Shikina

Contents

1. Introduction 845
2. Equilibrium properties of a charged dislocation in n-type semiconductors 848
2.1 Screening length; 2.2 Spectrum of electrons on a charged dislocation; 2.3 Determination of the filling factor
3. Charged dislocations in p-type semiconductors 855
3.1 Neutral model of the acceptor – donor action of dislocations; 3.2 Coulomb correction to the model; 3.3 Origin of an acceptor – donor level; 3.4 Inversion of the type of conduction in plastically deformed n-type semiconductors
3.5 Inversion of the type of conduction in germanium
4. Current-voltage characteristic of a sample with charged dislocations 863
4.1 Current – voltage characteristic of a barrier with saddle points; 4.2 Parameters of saddle points; 4.3 Influence of random fluctuations of the barrier profile; 4.4 Experiments on dislocation barriers; 4.5 Current – voltage characteristic of a single charged dislocation in a semiconductor
5. Relaxation phenomena 872
5.1 Exponential relaxation; 5.2 Logarithmic relaxation
6. Conclusions 874
References 875

Abstract. The current status of the subject of charged dislocations in germanium and silicon semiconductor crystals is discussed. Equilibrium properties of plastically deformed germanium and silicon are described by a phenomenological model of the electron spectrum of charged dislocations in these crystals. This model is a development of the Shockley – Read theory and it postulates two acceptor levels, E_1 and E_2, and also one donor level, $\mathcal{E}_1$. Moreover, it is necessary to introduce a finite capacity C_1 of the acceptor level E_1. The adopted model provides a self-consistent description of the main electrical properties of plastically deformed germanium and silicon. These properties include the conductivity of the crystals in the n and p states, details of inversion of the type of conduction caused by dislocations, some features of the current – voltage characteristics of crystals with oriented sets of dislocations, simplest relaxation phenomena, etc. In germanium, the level E_1 is located near $E_1 \approx 0.1$ eV above the top of the valence band and its capacity is $C_1 \lesssim 0.1$. The corresponding parameters of silicon are $E_1 \approx 0.4$ eV and $C_1 \lesssim 0.1$. It is worth noting the smallness of the capacity C_1, which justifies inclusion of this additional parameter among the characteristics of the electron spectrum of dislocations.

V B Shikin Institute of Solid-State Physics, Russian Academy of Sciences, 142432 Chernogolovka, Moscow Province
Fax: (096) 517-19-49
E-mail: shikin@issp.sherna.msk.su;
Yu V Shikina Institute of Microelectronics Technology and High-Purity Materials, Russian Academy of Sciences, 142432 Chernogolovka, Moscow Province

Received 16 November 1994; revision received 27 February 1995
Uspekhi Fizicheskikh Nauk **165** (8) 887 – 917 (1995)
Translated by A Tybulewicz

1. Introduction

The main ideas on a possible role of dislocations in determination of the electric properties of semiconductor crystals were put forward in the fifties during the period of remarkable progress in the physics of semiconductors. The first experimental results, demonstrating clearly a significant influence of dislocations on electric properties of semiconductors, were obtained by Gallagher [1] who showed that plastic deformation of germanium and silicon increases their resistivity and reduces the minority-carrier lifetime.

The experimental results of Gallagher [1] and a simple atomic model of a dislocation core in a covalent crystal were used by Shockley [2] to put forward a fruitful idea of the existence, along a dislocation, of what are known as dangling bonds that can exhibit acceptor or donor properties. Shockley's idea was developed quantitatively by Read [3, 4]. Read formulated the main propositions of a phenomenological theory of charged dislocations: he introduced the concept of dislocation electron levels E_i, the filling factor f† of dislocation levels, the radius R of a Read cylinder surrounding each charged dislocation and

†*Translator's note.* Read called this quantity 'the fraction of the occupied states'; other authors use 'the occupation ratio', etc.

screening the linear charge localised on it, etc. Read's work revealed clearly the main feature of the occupation of electron dislocation levels by free electrons. In contrast to the problem of occupation of point centres, in the case of dislocations this problem should be solved taking account of the Coulomb interaction of electrons which settle on a dislocation and of the self-consistent influence of this interaction on the quantity f.

The work of Shockley and Read [2–4] and the subsequent experiments (Refs [5, 6]) reporting anisotropy of samples with a set of oriented dislocations has determined the 'language' and the main physical parameters of the problem. Although the general picture is now much more complex compared with the initial variant discussed by Read [3, 4], the importance of this early work has not diminished with time.

Extensive experimental and theoretical investigations of various details of the behaviour of charged dislocations in semiconductors, which have followed Refs [1–4], have been summarised on many occasions in a number of interesting reviews. Among them one should mention particularly a chapter written by Labusch and Schroter [7] in *Dislocations in Solids* (Vol. 5) published in 1980 under the editorship of Nabarro, the review of Osip'yan (Ossipyan) [8] published somewhat later (1982), and the review of Matare [9]. The purpose of the present review is to consider the state of the problem of charged dislocations at the phenomenological level in the late eighties. In view of the rapidly growing volume of information, we shall ignore almost completely the properties of charged dislocations in II–VI semiconductors (which are discussed in an excellent manner in Ref. [10]) and also the spin-dependent effects, dealt with sufficiently thoroughly in Ref. [8].

In the development, at this stage, of a phenomenological description of the properties of charged dislocations in covalent semiconductors we must bear in mind the following repeatedly verified observations.

(1) Introduction of dislocations into n-type semiconductors reduces the average concentration of free carriers and the reduction becomes stronger as a result of cooling. In other words, dislocations act as acceptors in n-type semiconductors. A typical example of such an effect of dislocations on an n-type semiconductor is demonstrated in Fig. 1.

(2) The conductivity of samples with an oriented set of dislocations is anisotropic (Fig. 2), which is evidence of the linearity of these defects.

(3) An increase in the dislocation density above a certain critical value results in inversion of the type of conduction of a sample. Characteristically, such inversion is a fairly abrupt transition, which can be seen clearly in Fig. 3 illustrating the behaviour of the Fermi level as a function of the plastic strain, i.e. of the dislocation density. The abruptness of the transition indicates that a dislocation has at least two acceptor levels, the lower of which is located near the top of the valence band. It is also important to note that inversion appears not when $n_d \approx n_D$, where n_d and n_D are the effective volume concentrations of donors and dislocation acceptor centres ($n_D = N_D a^{-1}$; N_D is the two-dimensional dislocation density; a is the atomic spacing), but under the conditions when $n_d \approx 10^{-2} n_D$. This circumstance has to be taken into account in the selection of the model of the lower acceptor level in the spectrum of electrons on a dislocation.

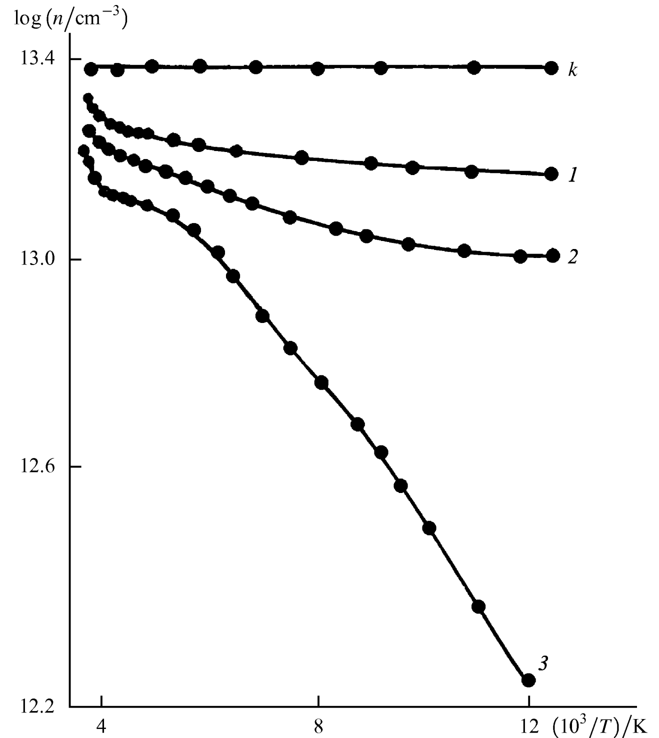

Figure 1. Temperature dependences of the electron density in plastically deformed germanium [8]. Here, curve k represents a control sample with a donor concentration $n_d = 2.9 \times 10^{13}$ cm^{-3}; curves *1*, *2*, *3* represent samples deformed to different degrees and characterised by dislocation densities of 2.8×10^6, 4.4×10^6, and 6×10^6 cm^{-2}, respectively.

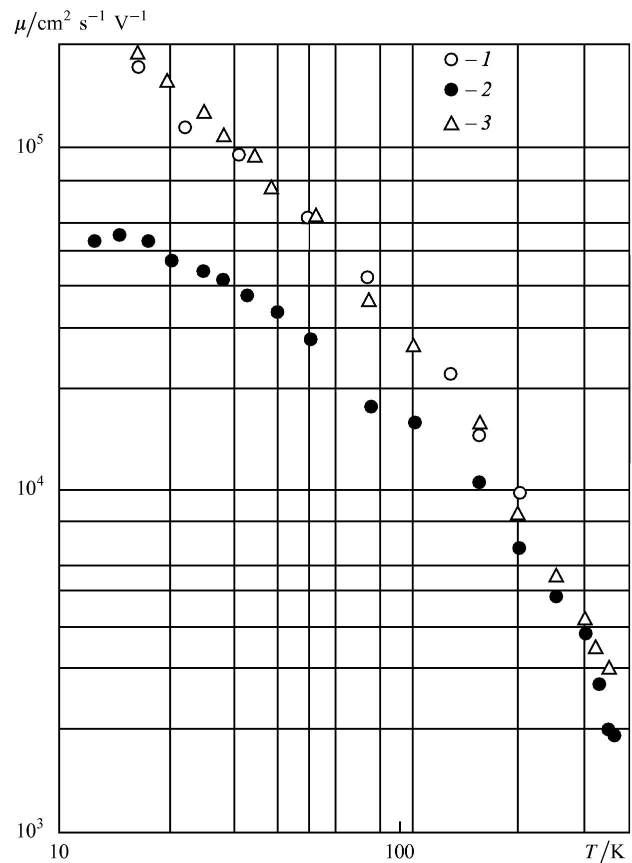

Figure 2. Dependences of the carrier mobility on temperature T [5]: (*1*) $I \| D$; (*2*) $I \perp D$; (*3*) control measurements.

(4) Dislocations exhibit acceptor – donor properties in p-type semiconductors. After introduction of dislocations the Hall concentration of holes can be lower or higher than the concentration of free carriers in a free sample, which is evidence of the acceptor – donor action of dislocation states in a p-type semiconductor. A typical example of such behaviour of free holes in a deformed sample is given in Fig. 4.

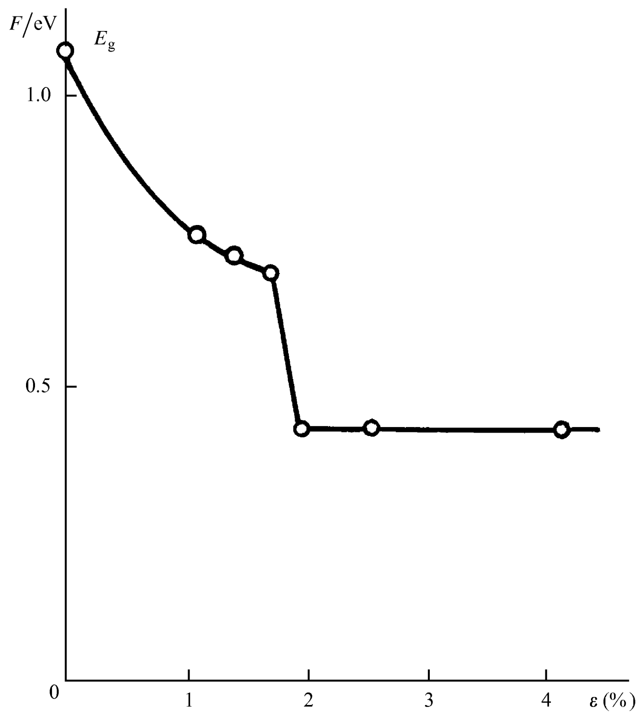

Figure 3. Behaviour of the Fermi level F, plotted as a function of the plastic strain of silicon crystals [8, 28].

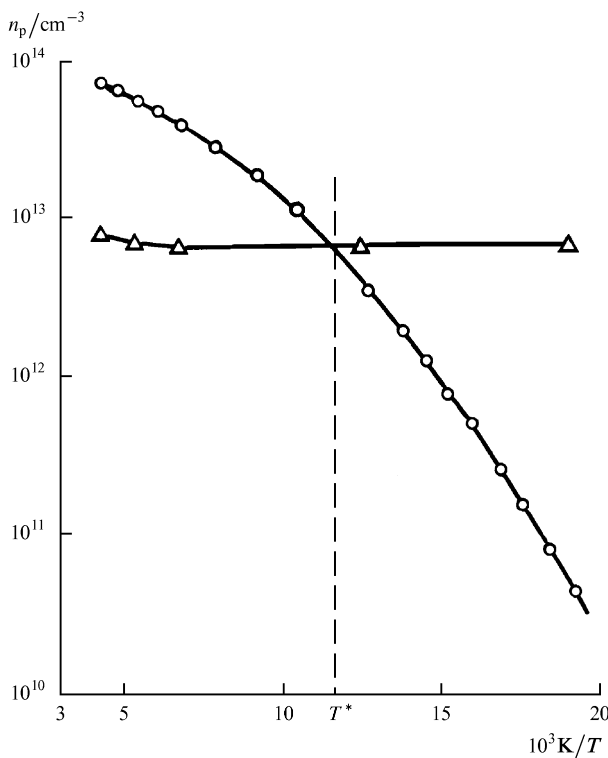

Figure 4. Hole concentration n_p in control (△) and plastically deformed (○) p-type germanium [7, 25], plotted as a function of T^{-1}; acceptor concentration $n_a = 7.3 \times 10^{12}$ cm^{-3} and dislocation density $N_D = 4.6 \times 10^7$ cm^{-2}

(5) There is a qualitative analogy between the behaviour of charged dislocations in germanium and the behaviour in silicon. The analogy is not absolute, for example, in the case of the spin-dependent properties (an ESR signal of dislocation origin is observed for silicon but not for germanium). However, in respect of the electric properties the similarity between germanium and silicon is quite close.

These observations determine the degree of complexity of a phenomenological model of a charged dislocation which can claim to provide a self-consistent description of the main observed effects involving charged dislocations. These dislocations are linear defects with deep discrete acceptor levels E_i and donor levels $\mathcal{E}_i$ in the band gap of a semiconductor. The positions of these levels are shown schematically in Fig. 5. All the energies are measured from the top of the valence band. The positions of the main acceptor E_1 and donor $\mathcal{E}_1$ levels are practically identical. This follows from Fig. 4 which shows that the slope of the temperature dependence of the concentration of holes in a deformed sample is practically unaffected on transition from the donor to the acceptor action of dislocations, i.e. by transition across a temperature $T = T^*$.

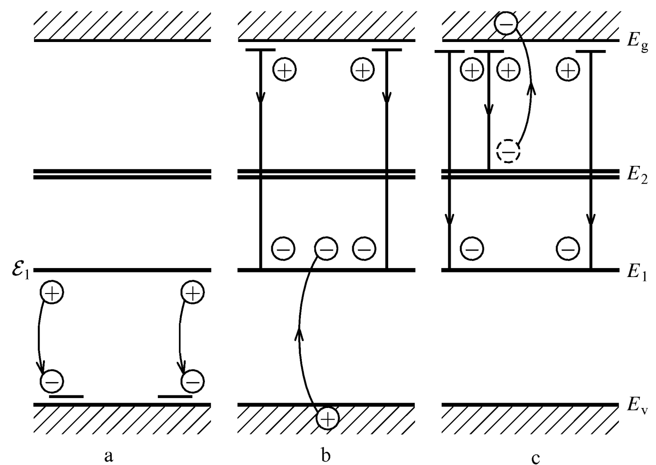

Figure 5. Energy level scheme of electrons localised at a 60° dislocation in germanium and silicon (a, b, and c show different electron transitions).

The special nature of the inversion of the type of conduction of a deformed sample with increase in the dislocation density N_D (see Fig. 3) makes it necessary to assume that the main acceptor level E_1 is of limited capacity $C_1 < 0.1$. To ensure a unified approach, we shall assume that all other dislocation levels have specific capacities C_i. It will be shown later that the existence of finite capacities C_i is also sufficient for the observation of various dislocation levels in the spectrum obtained by the DLTS (deep level transient spectroscopy) method. Naturally, introduction of finite capacities C_i is not the only possible way of filling of higher dislocation levels with electrons. In principle, the

same properties may be expected of a model which takes account of the free motion of electrons along a dislocation axis which leads to a finite energy of zero-point vibrations along a dislocation. However, this theoretical variant cannot account for the abruptness of the transition illustrated in Fig. 3.

One of the tasks of our review will be to demonstrate that the proposed model is not in conflict with the various experiments carried out on n- and p-type samples. We shall assume that the parameters $\mathcal{E}_i$, E_i, C_i, and if necessary also S_i (S_i are the capacities of donor levels) are found experimentally and are reasonably reproducible between one set of experiments and another.

2. Equilibrium properties of a charged dislocation in n-type semiconductors

As pointed out above, a specific feature of the problem of electron occupation of the dislocation levels is the need to include the Coulomb interaction between electrons that have settled on a dislocation. The foundation stone of Read's theory [3, 4] and of all its subsequent modifications is the correct account of this interaction and of its influence on the process of electron localisation. A systematic representation of this theory requires introduction of a number of specific definitions, which are used in the description of the equilibrium and simplest kinetic properties of charged dislocations.

2.1 Screening length

2.1.1 We shall assume that an n-type semiconductor with a donor concentration n_d contains, at temperatures corresponding to the complete ionisation of the donors, a charged filament with the filling factor f:

$$f = \frac{a}{c} \,. \tag{1}$$

Here, a is the lattice period along the dislocation axis and c is the average distance between electrons on a dislocation. The potential φ of a charged dislocation falls away from the axis because of the screening by the ionised donors. If over the whole region where $\varphi(\mathrm{r})$ is defined the inequalities

$$\frac{e\varphi}{T} \ll 1 \,, \quad 0 \leqslant r < \infty \tag{2}$$

are obeyed (T is the absolute temperature and r is the distance from the dislocation axis), the general Poisson equation

$$\Delta\varphi = \frac{4\pi e}{\varepsilon}(n_\mathrm{d} - n_\mathrm{e}) \,, \tag{3}$$

$$n_\mathrm{e}(r) = n_\mathrm{d} \exp\left(-\frac{e\varphi}{T}\right) \tag{3a}$$

may be linearised:

$$\Delta\varphi = \frac{4\pi e^2 n_\mathrm{d}}{\varepsilon T}\,\varphi \,.$$

Here, ε is the permittivity of the semiconductor. This equation becomes dimensionless as a result of substitution of the quantities

$$x = \frac{r}{r_\mathrm{D}} \,, \quad r_\mathrm{D}^2 = \frac{\varepsilon T}{4\pi e^2 n_\mathrm{d}} \,, \tag{4}$$

where r_D is the familiar screening length applicable to weak electrostatic fields, known as the Debye length.

2.1.2 In the problem of screening of a charged dislocation the situation is the reverse of that described above, because in a wide range of distances $0 < r \leqslant R$ from the dislocation axis the following inequality is obeyed:

$$\frac{e\varphi}{T} \gg 1 \,, \tag{5}$$

which is opposite to that in expression (2). If this range $r \leqslant R$ satisfies

$$R \gg r_\mathrm{D} \,, \tag{6}$$

then within this range we can simplify the problem still further by assuming that $n_\mathrm{e} \ll n_\mathrm{d}$. The Poisson equation then reduces to

$$\Delta\varphi \approx \frac{4\pi e^2 n_\mathrm{d}}{\varepsilon} \,. \tag{7}$$

The solution of Eqn (7) with the 'geometric' boundary condition

$$\left.\frac{\partial\varphi}{\partial r}\right|_{r=R} \approx 0 \tag{7}$$

and subject to the simplifying assumption $\varphi|_{r=R} \approx 0$ is as follows:

$$\varphi(r) = \frac{ef}{\varepsilon a}\left[2\ln\frac{R}{r} - \left(1 - \frac{r^2}{R^2}\right)\right] \,, \tag{8}$$

$$\pi R^2 n_\mathrm{d} = \frac{f}{a} \,.$$

The quantity R, defined by expression (8), was first introduced by Read [3, 4] and has since been called the Read radius. The physical meaning of this quantity is quite simple. In the geometric approximation, i.e. if $R \gg r_\mathrm{D}$, the quantity R is the distance at which the field of a charged dislocation is compensated by the field of ionised donors. Naturally, a full picture of the screening is more complex. However, if $R \gg r_\mathrm{D}$, we can usually ignore the Debye screening and consider only the Read screening.

The ratio of the Read and Debye lengths can be obtained from expressions (4) and (8):

$$\frac{R^2}{r_\mathrm{D}^2} = \frac{4e^2 f}{\varepsilon a T} \,. \tag{9}$$

This ratio is large if

$$\varGamma = \frac{e^2 f}{\varepsilon a T} \gg 1 \,. \tag{10}$$

In the real cases of germanium and silicon, when $f \leqslant 0.1$, the ratio defined above can reach $\varGamma \geqslant 10$. Under these conditions the Read screening mechanism is the dominant one.

It should be pointed out that, apart from the electrostatic forces between a dislocation and free electrons, there is also a deformation interaction $V_\xi(r, \theta)$ discussed in detail below. This interaction is not cylindrically symmetric:

$$V_\xi(r,\theta) = \frac{\mathrm{const}}{r}\sin(\theta) \,,$$

where θ is the angle measured from the glide plane of an edge dislocation. Therefore, the overall distribution of

electrons around a charged dislocation depends, in principle, on the angle θ. However, the deformation potential V_ξ decreases with distance as $1/r$, whereas the electrostatic potential $\varphi(r)$ given by expression (8) depends logarithmically on r. For this reason, at distances $r \approx R$, where a Read cylinder is formed, the deformation interaction can be ignored or it can be included by means of perturbation theory.

One more seemingly self-evident simplification has to be discussed separately. This is related to the role of holes in the determination of the properties of a charged dislocation in n-type semiconductors. The equilibrium concentration of holes far from a dislocation is exponentially small and its contribution to the charge distribution in the vicinity of a charged dislocation would seem to be negligible:

$$n_{\mathrm{p}} = n^*(T)\exp\left(-\frac{F}{T}\right) \ll n_{\mathrm{d}} \,. \tag{11}$$

Here $n^*(T)$ is the density of the hole states in the valence band and F is the Fermi level. However, holes are attracted to negatively charged dislocations and the attraction is not trivial. To deal with this, we shall calculate the total number of holes pulled into a Read cylinder:

$$N_+ = 2\pi\int_c^R n_{\mathrm{p}}\exp\left(\frac{e\varphi}{T}\right) r\,\mathrm{d}r$$

$$= 2\pi n_{\mathrm{p}}\int_c^R \left(\frac{R}{r}\right)^{2\Gamma}\exp\left[-\Gamma\left(1-\frac{r^2}{R^2}\right)\right] r\,\mathrm{d}r \,, \tag{12}$$

where $\varphi(r)$ is described by expression (8) and Γ by expression (10). The value of N_+ depends in a step-like manner on the parameter Γ. If $\Gamma < 1$, the integral in expression (12) is governed primarily by the distances $r \leqslant R$:

$$N_+ = \pi R^2 n_{\mathrm{p}}\exp(-\Gamma)\int_0^1 x^{-\Gamma}\exp(\Gamma x)\,\mathrm{d}x$$

$$= \pi R^2 n_{\mathrm{p}}\exp\left[-\Gamma\left(\frac{1}{1-\Gamma} - \Gamma\,\frac{\Gamma}{2-\Gamma}\right)\right] \,. \tag{12a}$$

In this limit the localisation of holes on a charged dislocation is unimportant.

However, if $\Gamma > 1$, the main part of the integral in expression (12) for N_+ is governed by the short distances $r \geqslant c$. As a result, expression (12a) should 'pass' across a singularity characterised by $\Gamma = 1$, and this corresponds to a step-like increase in N_+ in a narrow range of the parameter Γ. The presence of such a jump in the dependence on T may give rise to the effects discussed below.

2.1.3 The Debye and the Read simplifications of the Poisson equation for charged dislocations in an n-type semiconductor do not exhaust all the limiting cases encountered in experiments. For example, when electrons begin to settle at donors and the definition of $n_{\mathrm{e}}(r)$ given by expression (3a) becomes invalid, the range of the parameters describing this situation deserves special attention. In this case the structure of the transition region, matching the region of complete ionisation of donors in the vicinity of a dislocation to the unperturbed part of a crystal, differs considerably from the Debye case, so that we can speak in general of the third (in addition to the Debye and Read) variant of the screening of the field of a charged dislocation in an n-type semiconductor.

The details of this case can be considered if in solving the Poisson equation we go beyond the geometric approximation represented by expression (7a) in order to obtain information on the real behaviour of the potential $\varphi(r)$ in the transition region. In the case of complete ionisation of donors, i.e. when expressions (3) and (3a) apply, the solution of interest to us can be obtained as follows.

First of all, it is easily demonstrated that the general cylindrically symmetric solution given by expression (8) for $\varphi(r)$ near the boundary of a Read cylinder R has the asymptote:

$$\varphi(r) = \frac{2\pi e n_{\mathrm{d}} x^2}{\varepsilon} \,, \quad x = R - r \,, \quad x \ll R \,. \tag{13}$$

In the same approximation characterised by $x/R \ll 1$, the exact equation for $\varphi(x)$ in the transition region follows from expressions (3) and (3a):

$$\Phi'' = \left[1 - \exp(-\Phi)\right] \,, \quad \Phi' = \frac{\mathrm{d}\Phi}{\mathrm{d}\bar{x}} \,, \tag{14}$$

where

$$\bar{x} = \frac{x}{r_{\mathrm{D}}} \,, \quad \Phi = \frac{e\varphi}{T} \,, \quad r_{\mathrm{D}}^2 = \frac{\varepsilon T}{4\pi n_{\mathrm{d}} e^2} \,,$$

and r_{D} is the Debye radius when the electron concentration is $n = n_{\mathrm{d}}$.

The first integral of the above equation for Φ, with a constant of integration selected to ensure vanishing of the function Φ' in the limit $\Phi \to 0$, is

$$\Phi' = \sqrt{2}\left[\Phi - 1 + \exp(-\Phi)\right]^{1/2} \,. \tag{15}$$

Consequently, the dependence $\Phi(\bar{x})$ is given by the relationship

$$\int \frac{\mathrm{d}\Phi}{\left[\Phi - 1 + \exp(-\Phi)\right]^{1/2}} = \pm\sqrt{2}\,(\bar{x} + C) \,, \tag{16}$$

where C is an arbitrary constant.

We shall now assume that at large values of x the coordinate dependence of Φ, which follows from relationship (16), is identical with the coordinate dependence given by expression (13). Since in the range of high values of Φ relationship (16) becomes

$$\Phi = 0.5(\bar{x} + C)^2 \,, \tag{16a}$$

we find that the asymptotes of $\varphi(x)$ described by expression (13) and (16a) are identical if we assume that $C = 0$. In other words, the solutions for φ described by expressions (13) and (16) are matched asymptotically if the origin in solution (16) coincides with the geometric boundary $r = R$ of a Read cylinder.

In practical calculations it is convenient to substitute suitable limits in the integral in expression (16):

$$\int_{\Phi_{\mathrm{R}}}^{\Phi} \frac{\mathrm{d}\Phi}{\left[\Phi - 1 + \exp(-\Phi)\right]^{1/2}} = \pm\sqrt{2}\,\bar{x} \,, \tag{17}$$

where the constant Φ_{R} is defined by the condition

$$\int_0^\infty n(x, \Phi_{\mathrm{R}})\,\mathrm{d}x = \int_{-\infty}^0 \left[1 - n(x, \Phi_{\mathrm{R}})\right]\mathrm{d}x \,, \tag{17a}$$

$$n(x, \Phi) = 1 - \exp(-\Phi) \,.$$

The general ideas on the boundary of a Read cylinder make it possible to use the auxiliary definition of Φ_{R}^* in

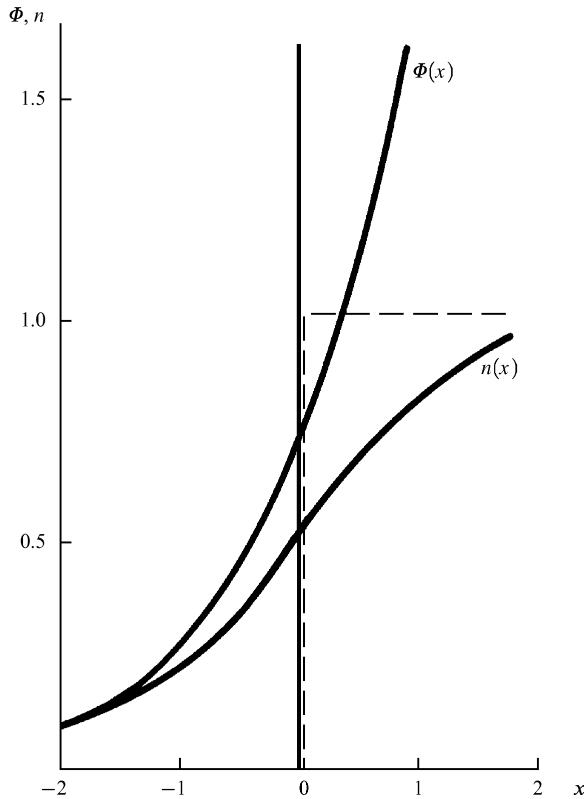

Figure 6. Behaviour of the Coulomb energy of free electrons Φ and of the concentration of ionised donors n in the vicinity of the boundary of a Read cylinder, which is represented by a dashed line. The local concentration $n(x)$ is reduced to the bulk concentration of donors n_d, x is in units of the Debye radius r_D, and the Coulomb energy $e\varphi$ is reduced to temperature ($\Phi = e\varphi/T$).

finding the value of Φ_R and in discussing other topics. This definition is $n(\Phi_R^*) = \frac{1}{2}$, where $n(\Phi)$ is the charge density relationship (17a). Written out explicitly, the definition of Φ_R is

$$1 - \exp(-\Phi_R^*) = \frac{1}{2} \,. \tag{18}$$

Hence, we have $\Phi_R^* = 0.693$. The correct value of Φ_R obtained from relationship (17a) and representing the electric potential on the surface of a Read cylinder is close to the definition of Φ_R^* given by expression (18).

Fig. 6 shows the dependences $\Phi(x)$ and $n(x)$ that follow from definitions (17), (17a), and (13). It is interesting to note that in the process of electron screening the real transition region is smeared out not over one but over five to six Debye radii.

Let us assume that the temperature of a sample is close to the freeze-out temperature of free electrons. In this limit the Fermi level is given by the expression [11]:

$$F^0 = -0.5\,E_d + 0.5\,T \ln \frac{n_d}{N_e} \,, \qquad N_e = \frac{2}{\hbar^3}\left(\frac{m^* T}{2\pi}\right)^{3/2} , \tag{19}$$

where m^* is the effective mass of an electron and E_d is a donor level measured from the bottom of the conduction band. N_e is the density of states in the conduction band. Consequently, the expression for the Fermi level in an external field becomes

$$F = F^0 - e\varphi \,. \tag{20}$$

The corresponding dimensionless equation for Φ, which replaces Eqn (14), is

$$\Phi'' = \left[1 - \frac{1}{1 + \alpha \exp \Phi}\right] - \alpha \exp(-\Phi) = n(\Phi) \,,$$

where

$$\alpha = \left(\frac{N_e}{n_d}\right)^{1/2} \exp\left(-\frac{E_d}{2T}\right) \ll 1 \,. \tag{21}$$

The first term on the right-hand side of the above equation represents the charge around a dislocation contributed by ionised donors in the field of a charged filament and the second term is the contribution made to the charge concentration by free electrons. In the limit $\Phi \to 0$, the right-hand side of Eqn (21) vanishes.

The first part of Eqn (21) is

$$\frac{(\Phi')^2}{2} = \ln \frac{1 + \alpha \exp \Phi}{1 + \alpha} + \alpha\big[\exp(-\Phi) - 1\big] \,. \tag{22}$$

The dependence $\Phi(\bar{x})$ is given by the relationship

$$\int_{\Phi_R}^{\Phi} d\Phi \left\{ \ln \frac{1 + \alpha \exp \Phi}{1 + \alpha} + \alpha\big[\exp(-\Phi) - 1\big] \right\}^{-1/2} = \pm\sqrt{2}\,\bar{x} \,, \tag{23}$$

where, as above, the constant Φ_R is found from the condition

$$\int_0^{\infty} n(\bar{x}, \Phi_R)\, d\bar{x} = \int_{-\infty}^{0} \big[1 - n(\bar{x}, \Phi_R)\big]\, d\bar{x} \,, \tag{24}$$

and $\Phi(\bar{x})$ is found from relationship (23).

The expression for $\Phi(\bar{x})$ given by relationship (23) can readily be investigated numerically in exactly the same way as has been done in the electron screening case discussed above (Fig. 7). However, in the present case the usefulness of the one-dimensional analysis is limited because the transition region is greatly smeared out and its one-dimensional description is no longer correct.

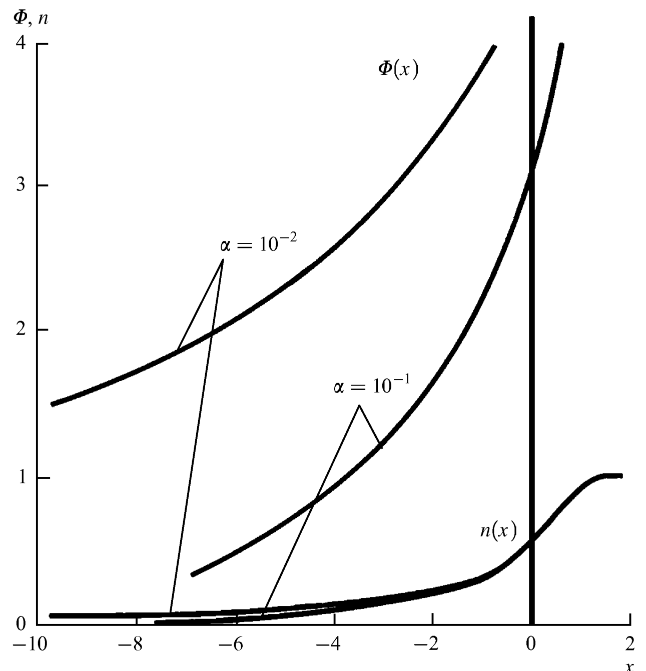

Figure 7. Dependences $\Phi(x)$ and $n(x)$ plotted for different values of α.

In an analysis of this situation it should be pointed out that Φ_R defined by the condition $n(\Phi_R) \approx 0.5$ is much greater than unity:

$$\Phi_R = \ln \frac{2}{\alpha} \gg 1 . \quad (25)$$

This circumstance distinguishes sharply the case of screening of the field of a charged filament by localised electrons from the screening by free electrons discussed above. In fact, in the localised electron screening a Read region, where all the donors are ionised, exists only if $\Phi \gg \Phi_R$. The general equation for this region [Eqn (21)] written down in terms of the cylindrical Laplace operator Δ becomes

$$\Delta\Phi = 1 . \quad (26)$$

A new region then appears which is not encountered at all in the screening by free electrons:

$$\Delta\Phi = 2\alpha \sinh(\Phi) , \quad \Phi_R \gg \Phi \geqslant 1 . \quad (27)$$

Only if $\Phi \leqslant 1$ does the potential Φ approach zero exponentially:

$$\Delta\Phi \approx 2\alpha\Phi . \quad (28)$$

It follows that the appearance of a new small parameter α in the problem greatly complicates the structure of the boundary of a Read cylinder.

The essential details of this limiting case are best considered, as in the initial variant of the description of the field around a charged filament [with a definition of $\varphi(r)$ given by expression (8)], by obtaining the final results of the distribution of the potential on the assumption of a step-like charge distribution around a charged filament:

$$n(r) = \begin{cases} n_d , & 0 \leqslant r \leqslant R_d , \\ n_e , & R_d \leqslant r \leqslant R_e , \end{cases} \quad (29)$$

where

$$n_e = n_d \alpha , \quad \alpha \ll 1 \quad \text{[see Eqn (21)]} .$$

The quantity n_e is the concentration of free electrons. The physical picture of such a distribution of the screening charge concentration is as follows. In the region $r \leqslant R_d$ all the donors are ionised. The radius of this region is set by the condition

$$e\varphi(R_d) \approx 0.5E_d . \quad (30)$$

However, a positive charge inside this cylinder is insufficient for total screening of the field of such a charged filament. Consequently, the filament field extends beyond the limits of the first jump in the charge concentration. In the region defined by $R_d \leqslant r \leqslant R_e$ the field amplitude is insufficient for complete ionisation of the donors. Therefore, the screening is then possible only because of the low concentration of free electrons $n_e \ll n_d$. Obviously, the distribution $n(r)$ described by expression (29) is not very close to the real smooth distribution of the charge concentration of Eqn (21). Nevertheless, it does have the necessary characteristic properties and it can be used to solve completely the cylindrically symmetric problem of the potential. The following boundary conditions are used to solve this problem:

$$\varphi(R_d + 0) = \varphi(R_d - 0) , \quad \varphi'(R_d + 0) = \varphi'(R_d - 0) ,$$
$$\varphi(R_e) = 0 , \quad \varphi'(R_e) = 0 , \quad (31)$$

which is supplemented by condition (30) that determines all the specifics of the situation.

A solution of the appropriate boundary-value problem gives the following final expression for R_e and the equation for the determination of R_d:

$$R_e^2 = \frac{R^2 - R_d^2}{\alpha} , \quad (32)$$

$$1 - x^2 = \frac{E_d}{2V_C \ln\left[\alpha^{-1}(1 - x^2)\right]} , \quad x = \frac{R_d}{R} , \quad (33)$$

$$V_C = e^2 n_d \varepsilon^{-1} \pi R^2 , \quad (34)$$

where R is the Read radius of the problem.

According to Eqn (33), the donor screening radius R_d is less than the Read radius R to the extent that the parameter $\gamma = E_d V_C^{-1}$ differs from zero. The electron radius R_e obeys $R_e \gg R$ if $\alpha \ll 1$.

Let us now consider the limitations of the donor screening theory. As pointed out above, the appearance of an additional step in the distribution of the charge concentration around a charged dislocation is due to the approach of the chemical potential to the value $F \to 0.5E_d$. This asymptote of F applies to a semiconductor with one type of impurity at temperatures as low as we please. If in addition to donors this sample contains only also a small amount n_a of an acceptor impurity, the chemical potential remains in the vicinity of $F \approx 0.5E_d$ only as long as $n_d \gg n_e \gg n_a$. Further cooling causes the chemical potential to approach the value $F \to E_d$ and the reasons for an additional step disappear. Therefore, the necessary conditions for the existence of an additional step are

$$n_d \gg n_e \gg n_a , \quad (35)$$

which may be obeyed in the vicinity of the freeze-out temperature of free electrons.

The one-dimensional description of the transition region is valid if

$$r_D^* = r_D \alpha^{-1/2} \ll R . \quad (36)$$

The definitions of R_d and R_e given by expressions (32) and (33) follow from the solution of the cylindrically symmetric problem. These definitions are reasonable if the first of the steps in the distribution $n(r)$ is sufficiently steep. Therefore, these relationships are valid only in the range of quite low temperatures and are basically qualitative, but they allow us to distinguish clearly between the quantities R, R_d, and R_e.

2.2 Spectrum of electrons on a charged dislocation

In the case of a shallow dislocation level the spectrum of electrons on a charged dislocation can be found by solving, in the one-band approximation, the relevant Schrodinger equation, which contains the initial attractive potential $V_D(r)$ of dislocation origin and the Coulomb field of a charged dislocation $V_C(r)$:

$$V_C(r) = e\varphi(r) , \quad \varphi(r) \text{ from solution (8)} ,$$
$$\left[\mathcal{E}(\hat{\boldsymbol{p}}) + V_D(r) + V_C(r)\right] \psi = E\psi , \quad (37)$$
$$\mathcal{E}(\hat{\boldsymbol{p}}) = \frac{\hbar}{2m_*} \Delta ,$$

where ψ is the wave function of an electron, m_* is the effective mass of an electron, Δ and $\hat{\boldsymbol{p}}$ are the Laplace and momentum operators. Examples of solutions of this

problem can be found in a number of theoretical papers, such as Ref. [12].

At first sight, an increase in the depth of an effective dislocation well seems to complicate the situation because the one-band approximation can no longer be used. However, we can say that this situation simplifies because we are not interested in a complete solution of the problem of the spectrum of electrons on a dislocation, but only in the deform-ation of this spectrum by the Coulomb interaction. The point is this: under the conditions of strong localisation of electrons on a dislocation, which in real semiconductors may be only a few interatomic spacings, the average Coulomb field near the axis of a charged dislocation is a much smoother function of the coordinate r than the effective potential energy $V_{\mathrm{D}}(r)$ of dislocation origin. In such a situation the initial equation (37), where $\mathcal{E}(\hat{\boldsymbol{p}})$ is now a complex function of the electron quasimomentum $\hat{\boldsymbol{p}}$, reduces to

$$\left[\mathcal{E}(\hat{\boldsymbol{p}})+V_{\mathrm{D}}(r)\right]\psi=\left[E_j(p_{\|})-V_{\mathrm{C}}(0)\right]\psi\,, \qquad (38)$$

where $V_{\mathrm{C}}(0)$ is the average value of the Coulomb energy in the vicinity of the axis of a charged dislocation and $E_j(p_{\|})$ are the eigenvalues of the wave equation (38) for an electron located on a charged dislocation. The index j in the definition of E_j labels the discrete quantum numbers corresponding to the transverse motion of an electron in the field $V_{\mathrm{D}}(r)+V_{\mathrm{C}}(r)$ and the momentum $p_{\|}$ represents the motion of an electron along the dislocation axis.

It follows from Eqn (38) that the problem of deep levels of an electron on a dislocation can be reduced to a problem free of the Coulomb interaction by new notation:

$$E_j(p_{\|})-V_{\mathrm{C}}(0)=E_j^0(p_{\|})\,, \qquad (39)$$

where $E_j^0(p_{\|})$ is the dispersion law of electrons on a dislocation in the absence of the Coulomb interaction. Therefore, the Coulomb interaction leads to a simple shift of the positions of all the deep levels by an amount

$$E_j(p_{\|})=E_j^0(p_{\|})+V_{\mathrm{C}}(0)\,. \qquad (40)$$

The separation between adjacent deep levels is not changed. Here, $V_{\mathrm{C}}(0)$ in formula (40) is $V_{\mathrm{C}}=e\varphi(c)$, where $\varphi(r)$ is obtained from expression (8).

The next problem, which has not yet been solved in a systematic manner, is the dependence of E_j on $p_{\|}$. The first indications of the existence of free motion of electrons along a dislocation in silicon were obtained from studies of the spin-dependent effects† reported in Refs [13, 14]. However, a general view on this topic has not yet been formulated.

In the absence of information on the nature of motion of dislocation electrons it is necessary to adopt some model assumptions to postulate free motion of an electron with an effective mass m_* along a dislocation or by postulating that the electrons are localised. However, it should be pointed out that the contribution of the longitudinal motion of electrons to the total free energy of dislocation electrons is proportional to temperature. On the other hand, in the case of deep dislocation levels and not-too-small filling factors the energies $E_j(0)$ and $V_{\mathrm{C}}(0)$ are much greater than the temperature. For this reason, in the calculation of the filling factor f of a dislocation the actual dependence $E_j(p_{\|})$ is important only at temperatures $eV_{\mathrm{C}}(0)<T$. In the other limiting case of $eV_{\mathrm{C}}(0)>T$, which has a wide range of validity in the case of deep levels, we can replace expression (40) with the approximate formula:

$$E_j(p_{\|})\approx E_j^0(0)+V_{\mathrm{C}}=E_j+V_{\mathrm{C}}\,. \qquad (41)$$

The quantities E_j are constants in this theory and should be determined experimentally.

Expressions (40) and (41) allow us to draw an important conclusion on the sequence in which the levels E_j become occupied. As long as only the lower level E_1 in the dislocation spectrum is filled, all the other levels should be vacant, since the rising value of V_{C} automatically lifts the higher levels with $j>1$ above the chemical potential. In view of this and since the feasibility of filling different dislocation levels has been confirmed experimentally (see, for example, Fig. 3), we have to assume that dislocation levels have finite capacities C_j which represent additional characteristics of the levels. We shall not try to calculate the values of these capacities or the positions of the dislocation levels in the band gap of a semiconductor, but we shall assume that each of the levels is characterised by two parameters E_j and C_j and their values should be found experimentally.

Until now in discussions of equilibrium properties of charged dislocations we have ignored completely the deformation phenomena which can influence the parameters of a charged dislocation. This gap will now be partly filled.

We shall begin by discussing the role of the deformation interaction between electrons (holes) and a dislocation. In the isotropic approximation this additional (to the Coulomb) interaction is described by

$$V_{\xi}^{i}(r,\vartheta)=W_i\,\frac{(1-2\nu)}{2\pi(1-\nu)}\,\frac{|\boldsymbol{b}|}{r}\,\sin(\vartheta)\,, \qquad i=l,p\,, \qquad (42)$$

where $\boldsymbol{b}$ is the Burgers vector; W_i are the electron–phonon interaction constants which are of the order of $W_i\approx 10$ eV for germanium [11] and are in principle different for electrons and holes; ν is the Poisson ratio; ϑ is the angle measured from the dislocation glide plane. Since the energy $V_{\xi}(r,\vartheta)$ of expression (42) is a variable-sign quantity, we can assume that there are quasimacroscopic regions in the valence and conduction bands near which electrons (holes) are attracted or repelled by dislocation.

Naturally, bound electron and hole states can appear in the potential described by expression (42). In the absence of cylindrical symmetry the details of the deformation spectrum of electrons and holes on a dislocation can be revealed only numerically. Calculations [16–21] give the following estimates of the 'depth' of the main deformation level E_{ξ} in germanium:

$$E_{\xi}^{\mathrm{e}}\simeq -0.1\ \text{eV}\quad \text{for electrons}\,,$$
$$E_{\xi}^{\mathrm{p}}\simeq +0.02\ \text{eV}\quad \text{for holes}\,. \qquad (43)$$

Such energies can still be regarded as representing 'shallow' levels and this justifies the one-band approximation in the calculation of $E_{\xi}^{\mathrm{e,p}}$.

It is interesting to note that the relative depth of a deformation well for holes in the vicinity of a charged dislocation may vary with the degree of electron occupation of the dislocation levels. As f increases, the electrons that have settled on a dislocation begin additionally to compress the lattice in accordance with the familiar propositions of

†It had been found subsequently that the Lomer dislocations [15] participated in the experiments described in Refs [13, 14].

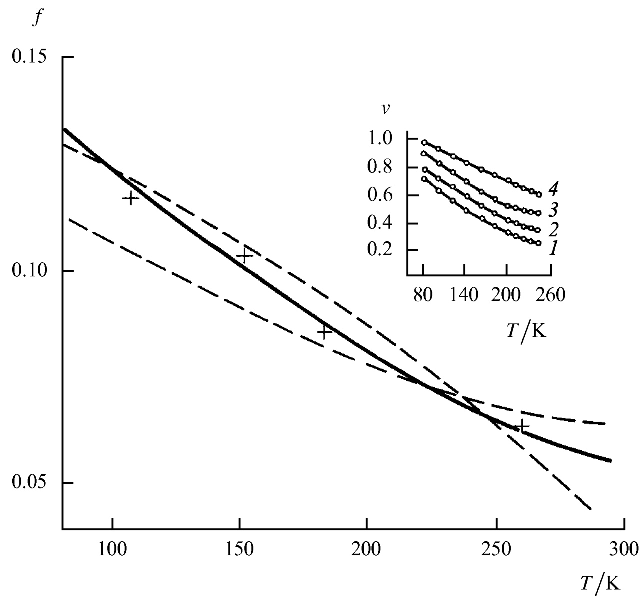

Figure 8. Different variants of an analysis of the experimental data of Ref. [23] for $f(T)$. The dashed curve represents the Read approximation characterised by $E_1 = E_2$, $E_2 + V_C = F$, and $E_2 = 0.34$ eV with the chemical potential F from Ref. [23]. The chain curve corresponds to the definition of $f(T)$ given by expression (47) for a model with two levels: $E_2 = 0.41$ eV, $C_2 = 0.1$, $E_1 = 0.1$ eV, $C_1 = 0.05$. The continuous $f(T)$ curve is calculated on the basis of expression (47) with the same two levels, but with the additional deformation contribution. The crosses are the experimental values taken from Ref. [23] The inset shows the temperature dependence of the fraction of the volume v occupied by dislocation cylinders and calculated from expression (52) for samples *1–4* with the following dislocation densities $N_D = 3 \times 10^6$, 3.8×10^6, 5.2×10^6, and 6×10^6 cm^{-2}, respectively; $n_d = 2.8 \times 10^{13}$ cm^{-3}.

the deformation potential theory. As a result, the energy of a single electron on a dislocation decreases by an amount [11]

$$\tilde{V}_\xi \approx W_0 \operatorname{div} \boldsymbol{u} \simeq \frac{W_0^2 f}{k\pi a^3} , \tag{44}$$

where the constant W_0 is analogous to that used in expression (42), k is the shear modulus, and a is the atomic spacing. The existence of an elastic strain proportional to f within a tube of radius a/f also deforms, in principle, the lattice outside the dislocation. However, actual calculations show that this effect can be ignored. The influence of the interaction described by expression (44) on the value of f is demonstrated in Fig. 8 (continuous curve).

One further elegant effect of deformation origin has not yet been confirmed experimentally, but it is worth attention and it should be taken into account in calculations preceding the planning of various future experiments on electrons at dislocations. The effect in question is the self-localisation of an electron which occupies a dislocation level and is, in principle, free to move along the dislocation axis. In reality, this does not occur because the deformation interaction described by expression (44) begins to play its part. This interaction has the effect that, in the one-dimensional motion which applies in this case, it is preferable for an electron to become self-localised in some specific scale along the dislocation axis. The result is the motion not of a free electron along a dislocation but of a polar quasiparticle with a significantly renormalised (by the deformation interaction) mass. Such a quasiparticle, first investigated for the localisation of electrons on a dislocation by Voronov and Kosevich [22], is called a condenson.

A standard method for demonstrating such one-dimensional localisation is as follows. The total functional of the energy of an electron on a dislocation takes account of its interaction with the lattice deformation, is minimised, and averaged over the transverse motion of an electron. The functional obtained after these steps leads to the following one-dimensional equation of electron motion:

$$\frac{\hbar^2}{2m_*}\chi'' - \lambda\chi + \alpha\beta^2\gamma^2\chi^3 = 0 ,$$

where

$$\int |\chi| \, dz = 1 , \tag{45}$$

$$\alpha \approx 0.003 , \quad \beta = \frac{W^2}{G} , \quad \gamma = \frac{2mWb\,(1-2\nu)}{2\pi\hbar^2(1-\nu)} .$$

Here, W is defined by expression (42); G is the Young modulus, α is a numerical constant which appears in the course of averaging over the transverse variables, and λ is the energy.

The normalised solution of Eqn (45), of interest to us, is

$$\chi(z) = \sqrt{0.5k}\,\cosh^{-1}\left[k(z - z_0)\right] , \quad k = \frac{m_*\alpha\beta^2\gamma^2}{8\hbar^2 G^2} . \tag{46}$$

Therefore, an electron becomes self-localised in the course of its motion along the axis of a charged dislocation.

2.3 Determination of the filling factor

A discussion of the equilibrium properties of charged dislocations should be completed by a calculation of the equilibrium filling factor f of a single dislocation, carried out for different limits in respect of the absolute temperature, the concentration of point defects, and the strain of a sample, We shall do this for n-type samples relying effectively on the information presented in Sections 2.1 and 2.2. If the problem is cylindrically symmetric and the finite mass of an electron moving along the dislocation axis is ignored, and if the inequality $R < N_D^{-1/2}$ is obeyed, the expression for f is

$$f = \sum f_j , \quad f_j = C_j\left[\exp\left(\frac{E_j + V_C - F}{T}\right) + 1\right]^{-1} , \tag{47}$$

$$j = 1, \ldots, J .$$

Here, F is the current value of the chemical potential, $V_C \simeq e\varphi(c)$, $\varphi(r)$ is defined by expression (8), the energy E_j and the chemical potential are measured from the top of the valence band, J is the maximum serial number of the dislocation levels, and N_D is the dislocation density. If the number of dislocations is small so that the Read cylinders of the individual dislocations do not overlap, i.e. if $R < N_D^{-1/2}$, then F can be the value of F for a dislocation-free n-type sample.

If the number of dislocation levels is unity ($J = 1$) and if $C_1 = 1$, the definition of f given by expression (47) reduces to the procedure employed in Read's papers [3, 4]. Then, with logarithmic precision, we can simplify the definition of f additionally by assuming that

$$E_1 + V_C = F . \tag{48}$$

Relationship (48) is equivalent to the Read equation:

$$E_1 + \frac{e^2 f}{\varepsilon a}\left(2\ln\frac{R}{c} - 1\right) = F\,, \tag{49}$$

which was derived in Read's first papers on the theory of charged dislocations [here, c has the same meaning as in expression (1)].

As the temperature T of a sample is increased, the vanishing of the exponential argument in the denominator of the Fermi function becomes a poor approximation even in the case when only one level is present. The general definition

$$f = C_1\left[\exp\left(\frac{E_1 + V_C - F}{T}\right) + 1\right]^{-1} \tag{50}$$

can be reduced to a form convenient for comparison with Eqn (49):

$$E_1 + V_C = F^*\,, \qquad F^* = F + T\left(\ln\frac{C_1}{f} - 1\right)\,. \tag{51}$$

It is obvious that the definition of f given by expression (51) has a structure similar to that given by Eqn (49), but the value of F^* is renormalised.

In general, $J > 1$, and there is only one correct way of calculating f, which is to use general expression (47).

Practical information on f can be derived from a variety of experiments. The most popular method involves measurement of the Hall effect in deformed samples [6, 23]. It is assumed that the Hall effect measurements give direct information on the average concentration of free carriers (electrons and holes) $\langle n_e \rangle$, which is related to the actual concentration n_e and the relative volume v of the Read cylinders $v \approx \pi R^2 N_D$ by (see Ref. [9]):

$$\langle n_e \rangle = n_e(1 - v)\,, \qquad v = \pi R^2 N_D\,. \tag{52}$$

If $\langle n_e \rangle$ and n_e are known, the value of v is readily estimated. The measured value of N_D can then be used to find R and, therefore, $f = \pi R^2 N_D a$. The inset in Fig. 8 shows the experimental values of v obtained by this method [23].

If the dislocations introduced into a sample are sufficiently collinear, the information on the parameter v can be obtained by measuring the conductivity of the sample along and across the direction of these dislocations, because we then have

$$\begin{aligned}\sigma_{\|} &= \sigma_0(1 - v)\,,\\ \sigma_{\perp} &= \sigma_0(1 - v)\,g(v)\,,\end{aligned} \tag{53}$$

where σ_0 is the conductivity of a control sample and $g(v)$ is a structure factor that takes into account the bypassing of the Read cylinders by free electrons.

In the experiments reported in Ref. [23] the degree of this anisotropy of the dislocation distribution was of the order of 1 : 5, so that it was reasonable to use the definitions described by the set of expressions (53). The results of such determination of f with the aid of these expressions give values plotted in Fig. 8.

The dependence $f(T)$ and the value of f described by expression (47) can be used to find the parameters of the spectrum of electrons on a dislocation. Fig. 8 includes some theoretical curves deduced subject to various approximations:

— a dashed curve obtained with the aid of relationship (48) on the assumption that there is one level $E_1 = E_2 = 0.34$ eV;

— a chain curve obtained in the approximation of two levels and on the basis of general expression (47).

It is worth noting that variation of the position of the level E_1 and of its capacity cannot increase the slope of the theoretical curve so as to reduce the discrepancy between the calculations and experiments.

The continuous curve in Fig. 8 is plotted in the approximation of two levels taking account of the deformation interaction represented by $\tilde{V}_\xi$, defined by expression (44), on the assumption that the wave function of an electron localised at a dislocation is smeared out over a distance of 9 Å.

The different calculated curves located close to the experimental points demonstrate that determination of the value of f on the basis of the transport of properties gives results which are far too ambiguous for determination of the characteristics of dislocation levels. They should be supplemented by DLTS experiments, by information on the behaviour of p-type germanium, or by some optical measurements which can be interpreted in a consistent manner.

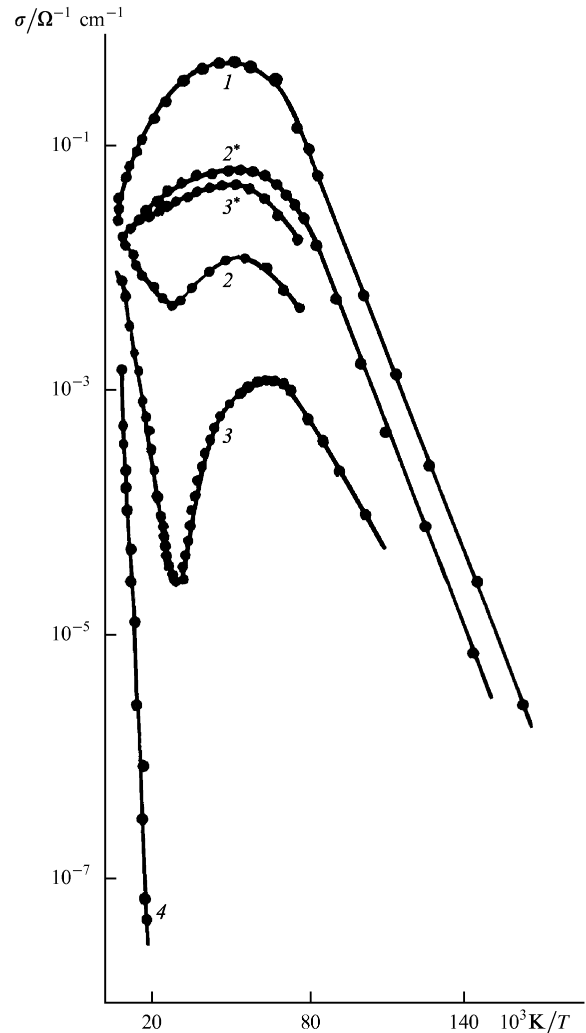

Figure 9. Temperature dependences of the electrical conductivity of control (*1*) and deformed (*2–4*) samples obtained in an electric field directed along (curves *2** and *3**) and across (curves *2–4*) the preferential direction of dislocations. The dislocation densities in samples *2–4* were 3.0×10^6, 3.8×10^6, and 5.2×10^6 cm^{-2}, respectively [24].

It is worth pointing out that the behaviour of the parameter v for silicon has not yet been investigated in the range $v < 0.5$.

We shall conclude our discussion of the experimentally observed effects demonstrating the presence of charged linear defects in plastically deformed semiconductors by noting an excellent qualitative result obtained very early on [5] in a study of the influence of oriented dislocations on the conductivity of a crystal, investigated subsequently in greater detail [24]. We are speaking here of a strong increase in the anisotropy of a semiconductor containing dislocations when its temperature T is reduced below a certain critical value T_0 (Fig. 9).

A qualitative explanation of this effect is as follows: when the temperature $T = T_0$ is reached, the Read cylinders of adjacent dislocations come into contact and the flow of the current in the direction normal to the dislocation axes becomes difficult. Therefore, the position of the point T_0 can be estimated from

$$R(T_0) \approx N_{\mathrm{D}}^{-1/2} , \qquad (54)$$

where N_{D} is the dislocation density in the semiconductor. If the dislocation density changes, this should alter the temperature T_0 in accordance with the estimate given by expression (54) and in accordance with the definition of the Read radius

$$\pi R^2 n_{\mathrm{d}} = \frac{f}{a} ,$$

where the filling factor varies approximately linearly with temperature (Fig. 8). The measurements reported in Ref. [24] confirm that the temperature T_0 decreases on reduction in the dislocation density, in accordance with expression (54).

3. Charged dislocations in p-type semiconductors

Let us now turn to p-type semiconductors. As first noted by Schroter [25], dislocations formed in p-type germanium have simultaneously both acceptor and donor properties. This follows from the experimental temperature dependence of the concentration of free holes in samples before and after plastic deformation (Fig. 4). At temperatures $T < T^*$, the concentration of free holes n_{p} in a deformed sample is less than the corresponding density in an undeformed control sample n_{p}^0, which can be explained by the donor action of the dislocations. At temperatures $T > T^*$, the reverse is true: we now have $n_{\mathrm{p}} > n_{\mathrm{p}}^0$, which indicates the acceptor action of dislocations in a semiconductor.

An analysis of Schroter's results [25] and of those reported later [26–28] has been made with the use of minimum information on the properties of charged dislocations in p-type semiconductors. It has been assumed specifically that at $T = T^*$, when dislocations are neutral, the Fermi level F coincides with the positions of a dislocation level E_0:

$$F(T^*) = E_0 . \qquad (55)$$

At first sight this hypothesis seems reasonable and it allows us to estimate E_0 (according to Refs [25–27], in the case of germanium we have $E \approx 0.09$ eV above the top of the valence band). However, a number of questions of qualitative importance remain unanswered. First of all, what is the nature of the level E_0: acceptor or donor? How can the vanishing of the filling factor f of dislocation levels under the conditions described by expression (55) at a finite temperature $T = T^*$ be explained? There is no doubt that this occurs (at $T = T^*$ the concentrations of holes in the deformed and control samples are identical, indicating the absence of excess electrons at dislocations), but its interpretation is not clear. Finally, a less obvious question: can the model of a charged dislocation with one phenomenological parameter, which is the position E_0 of a dislocation level in the band gap of a semiconductor, describe satisfactorily the properties of $n_{\mathrm{p}}(T)$ at high temperatures $T \gg T^*$? In fact, we can assume that in this range of temperatures T the dislocations act as acceptors. Under the conditions such that $T \gg T^*$ the average concentration of holes $n_{\mathrm{p}}(T)$ in a deformed sample is much higher than the concentration of holes n_{p}^0 in a control sample, so that in discussing the situation at $T \gg T^*$ we can ignore the concentration of point acceptors. As a result, the question of the electron occupation of a dislocation and, in particular, the solution of the appropriate electrostatic problem, reduces to a description of the interaction between a negatively charged dislocation and a cloud of holes surrounding it.

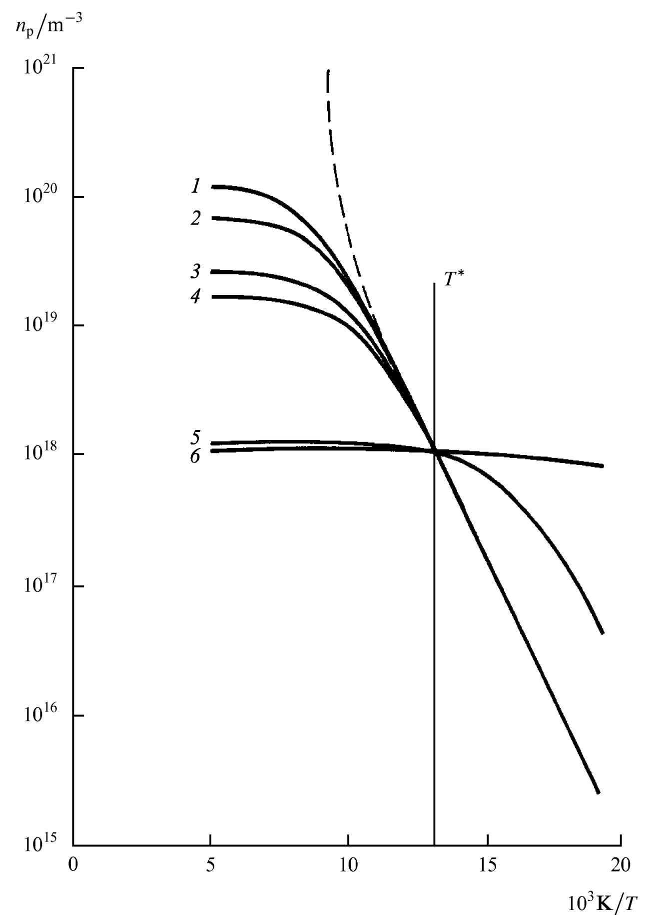

Figure 10. Behaviour of $n_{\mathrm{p}}(T)$ in the neutral approximation for $E_1 = \mathcal{E}_1 = E_0$, $S_1 = 1$. The parameters E_0 and C_1 were determined from the experimental [27] position of $T = T^*$ and from the slope of the $n_{\mathrm{p}}(T)$ curve at this temperature. This gave $E_0 = 0.077$ eV, $C_1 = 0.144$. Curves *1–6* correspond to the dislocation densities 3.5×10^{11}, 2×10^{11}, 7×10^{10}, 4.5×10^{10}, 10^9, and 10^7 m^{-2}. The dislocation densities N_{D} for curves *1–4* were taken from Ref. [27].

The electrostatic problem formulated above has an exact solution [29, 30]. We shall omit the details of the calculations, which can be found in Ref. [30], and give only the final expression for the average hole concentration:

$$\tilde{n}_{\mathrm{p}}(T)=\frac{1}{aR^2}\frac{T}{T_{\mathrm{C}}}\,,\qquad T_{\mathrm{C}}=\frac{e^2}{\varepsilon a}\,,\qquad T^*<T<T_{\mathrm{C}}\,. \tag{56}$$

Here, a is the atomic spacing, ε is the permittivity of the semiconductor, and R is the average distance between the dislocations.

We can easily see that the predictions following from expression (56) are in qualitative conflict with the observations [26, 27], which can be seen from Fig. 10 where the dependence $\tilde{n}_{\mathrm{p}}(T)$ described by expression (56) is represented by the dashed curve. This conflict can be removed in only one way: we have to assume that the electron occupancy of a dislocation level is limited not only by the Coulomb forces [taken into account in the derivation of expression (56)], but also by other factors of nonelectric origin.

In view of this, it is necessary to complicate the model of the spectrum in order to describe the properties of a p-type semiconductor with a fairly high dislocation density:

(a) the spectrum should have two levels in the lower part of the band gap, an acceptor E_1 and a donor $\mathcal{E}_1$;

(b) the levels E_1 and $\mathcal{E}_1$ have finite capacities C_1 and S_1.

3.1 Neutral model of the acceptor – donor action of dislocations

If in addition to the assumptions (a) and (b) identified above, we also postulate that the dislocation density N_{D} is sufficiently high, then electrons (holes) settling on a dislocation hardly interact with one another and the statistics of a semiconductor with dislocations resembles a similar problem of doping by point-like impurities. In particular, we can use the condition of local neutrality [31], which is represented by the following equation for the Fermi level F:

$$N_{\mathrm{v}}(T)\exp\left(-\frac{F}{T}\right)+\frac{n_{\mathrm{d}}}{1+\exp\left[-(\mathcal{E}_1-F)/T\right]}=\frac{n_{\mathrm{a}}}{1+\exp\left[(E_1-F)/T\right]}+n_{\mathrm{a}}^0\,. \tag{57}$$

Here n_{a}^0 is the concentration of point acceptors; E_1 and $\mathcal{E}_1$ are the positions of the acceptor and donor levels in the band gap of the semiconductor; $n_{\mathrm{a}}=N_{\mathrm{D}}C_1/a$ and $n_{\mathrm{d}}=N_{\mathrm{D}}S_1/a$ are the effective concentrations of dislocation acceptors and donors; C_1 and S_1 are the corresponding capacities of the dislocation levels; $N_{\mathrm{v}}(T)$ is the density of the whole states in the valence band. The $n_{\mathrm{p}}(T)$ curve passes through the point $T=T^*$ without a kink, as found experimentally [25 – 27], if

$$E_1\cong\mathcal{E}_1=E_0\,. \tag{58}$$

We shall adopt this additional proposition and introduce the notation

$$x=\exp\frac{E_0-F}{T}\,,\qquad n_0=N_{\mathrm{v}}(T)\exp\left(-\frac{E_0}{T}\right)\,, \tag{59}$$

which modifies Eqn (57) to

$$n_0x+\frac{xn_{\mathrm{d}}}{1+x}=\frac{n_{\mathrm{a}}}{1+x}+n_{\mathrm{a}}^0 \tag{60}$$

or

$$x=-\frac{1}{2}\left(1+\frac{n_{\mathrm{d}}}{n_0}-\frac{n_{\mathrm{a}}^0}{n_0}\right)+\left[\frac{1}{4}\left(1+\frac{n_{\mathrm{d}}}{n_0}-\frac{n_{\mathrm{a}}^0}{n_0}\right)^2+\frac{n_{\mathrm{a}}}{n_0}+\frac{n_{\mathrm{a}}^0}{n_0}\right]^{1/2}\,. \tag{61}$$

In the case of interest to us we have

$$n_{\mathrm{d}}>n_{\mathrm{a}}\gg n_{\mathrm{a}}^0\,, \tag{62}$$

so that expression (61) simplifies to

$$x\approx\frac{n_{\mathrm{a}}+n_{\mathrm{a}}^0}{n_0+n_{\mathrm{d}}-n_{\mathrm{a}}^0}\,. \tag{63}$$

Hence, it is seen quite readily that in the limit $T\to\infty$, we obtain

$$n_0\gg n_{\mathrm{d}}\,,\quad x\to\frac{1}{n_0}\,(n_{\mathrm{a}}+n_{\mathrm{a}}^0)\,,\quad n_{\mathrm{p}}(T)=n_0x=n_{\mathrm{a}}+n_{\mathrm{a}}^0\,. \tag{64}$$

The asymptotic expression (64) for $n_{\mathrm{p}}(T)$ can be used to estimate the capacity C_1 from the known experimental values of $n_{\mathrm{p}}(\infty)$ and N_{D}. According to Ref. [26], we have $n_{\mathrm{p}}(\infty)=10^{20}\ \mathrm{m}^{-3}$ and $N_{\mathrm{D}}=3.5\times10^{11}\ \mathrm{m}^{-2}$, so that

$$C_1\approx0.13\,. \tag{65}$$

The point T^* is of interest, which in terms of the quantities defined by expressions (59) and (60) is described by the following equalities:

$$\begin{cases} n_{\mathrm{d}}x^*=n_{\mathrm{a}} & x^*=x(T^*)\,, \qquad (66\mathrm{a})\\ n_0x^*=n_{\mathrm{a}}^0\,, & n_0^*=n_0(T^*) \qquad (66\mathrm{b})\end{cases}$$

or

$$\frac{C_1}{S_1}=\frac{n_{\mathrm{a}}^0}{n_0(T^*)}\,. \tag{67}$$

Obviously, the value of T^* is independent of the dislocation density, i.e. all the dependences $n_{\mathrm{p}}(T)$ obtained for different dislocation densities should intersect at one point $T=T^*$, which is indeed true. Next, since the experiments reported in Ref. [27] do not suggest that S_1 is particularly small, we can assume that $S_1\approx1$. Then, expressions (66) and (67) provide the definition of the energy E_0:

$$x^*=\frac{C_1}{S_1}\quad\text{or}\quad E_0=F(T^*)-T^*\ln\frac{C_1}{S_1}\,. \tag{68}$$

The definition of E_0 given by the above expression is identical with expression (55) in the special case when $C_1=S_1$.

The slope of the dependence $n_{\mathrm{p}}(T)$ at the point T^* is

$$\left.\frac{\mathrm{d}n_{\mathrm{p}}}{\mathrm{d}(T^{-1})}\right|_{T=T^*}=\frac{E_0n_0^*n_{\mathrm{a}}}{n_0^*+n_{\mathrm{d}}}\left(\frac{n_0^*}{n_{\mathrm{d}}+n_0^*}-1\right)\,. \tag{69}$$

As N_{D} tends to zero, the slope naturally also tends to zero. However, numerically this dependence is too weak to account for the observed dispersion of the $n_{\mathrm{p}}(T)$ curves considered as a function of N_{D}. Fig. 10 gives the numerically calculated dependences $n_{\mathrm{p}}(T)$, plotted in Ref. [31] on the basis of the definition $n_{\mathrm{p}}=xn_0$ and of the expression (61) for x. These dependences agree well with the experimental results [26, 27] in a wide range of temperatures for dislocation densities N_{D} equal to 3.5×10^{11} and $2\times10^{11}\ \mathrm{m}^{-2}$, but they disagree in the

range $N_D < 7 \times 10^{10}$ m^{-2}. The reason for this disagreement may be the Coulomb interaction between charges on dislocations, because this interaction becomes stronger at lower dislocation densities.

3.2 Coulomb correction to the model

The asymptotic properties of the neutral model are considered above (Section 3.1) in the limiting case when $E_1 = \mathcal{E}_1$, $S_1 \to 1$. In general, it is necessary to use numerical methods. If we assume, as in Section 3.1, that $E_1 = \mathcal{E}_1$, $S_1 \to 1$, we obtain the dependence of the hole concentration n_p on T [32]. The small difference between the parameters E_0 and C_1 obtained from Fig. 10 and those deduced from analytic estimates (Section 3.1) is due to different methods of fitting the experimental data [27]. In Section 3.1 the temperature T^* and the asymptotic value of n_p are used at high temperatures. In Fig. 10 the fitting involves the value of T^* and the slope of the dependence $n_p(T)$ at T^*.

A shortcoming of the neutral model is a weak sensitivity of $n_p(T)$ to the dislocation density N_D in the range $N_D < N_D^*$, where N_D^* is the asymptotic value of N_D at which $n_p(T)$ ceases to depend on N_D. Naturally, as N_D tends to zero, the dependence $n_p(T)$ tends to the control value n_p^0 (Fig. 10). However, this dependence is insufficiently strong to explain the data reported in Refs [26, 27] for the range of small strains. The purpose of this section is to discuss possible factors that can increase the sensitivity of the model to the dislocation density. There are two such factors: the different depths of the levels E_1 and $\mathcal{E}_1$, and the Coulomb interaction between electrons that have settled on a dislocation.

3.2.1 The role of $2\Delta = E_1 - \mathcal{E}_1$ in the neutral model characterised by

$$E_1 = E_0 + \Delta\,, \quad \mathcal{E}_1 = E_0 - \Delta\,, \tag{70}$$

can be identified without introducing any additional concepts. We shall continue to use the system of definitions given in Section 3.1 or expressions (76) and (77) given below, from which the Coulomb corrections are removed. The behaviour of $n_p(T)$ expected for the

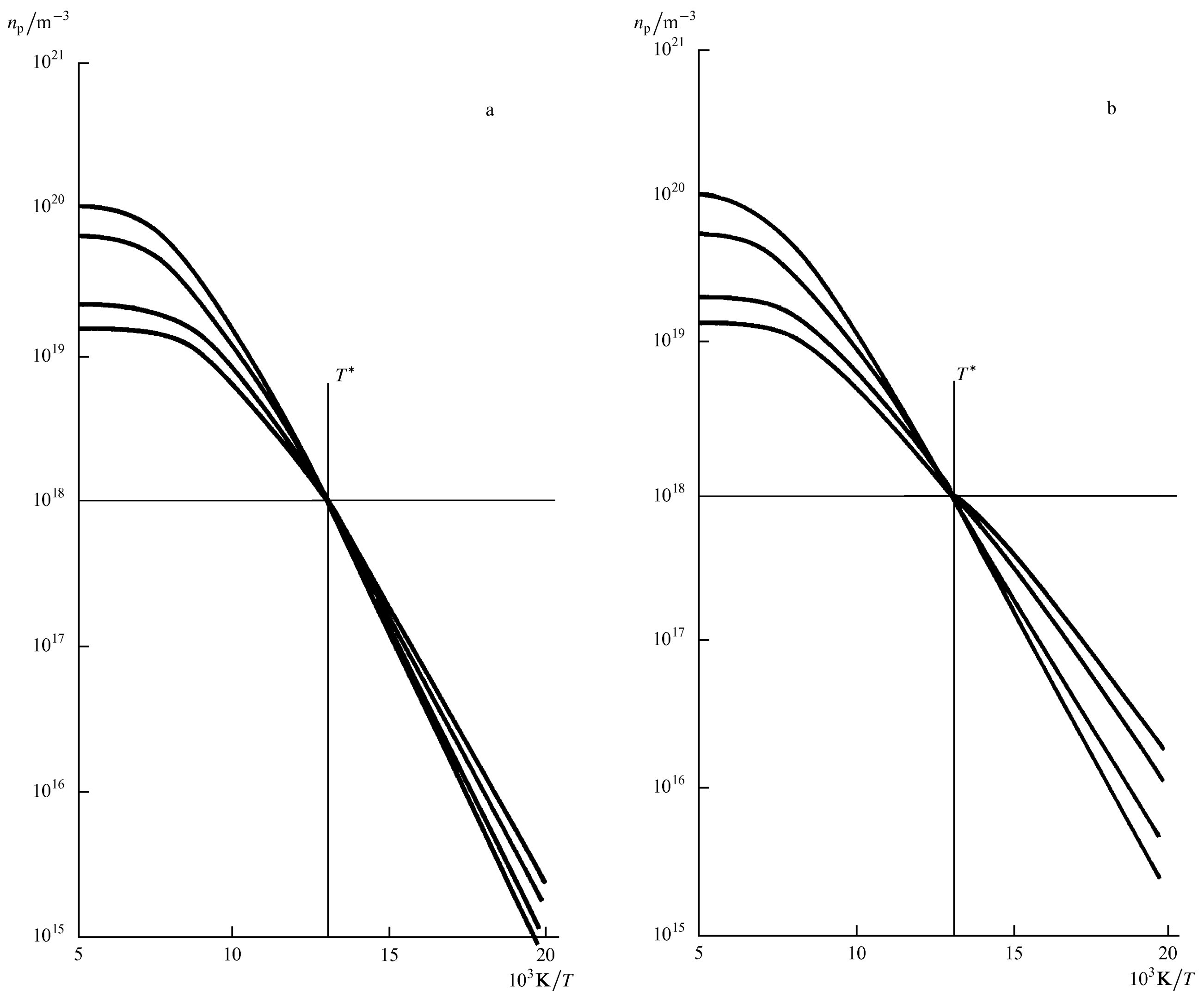

Figure 11. Influence of the parameters Δ/E_0 on the behaviour of $n_p(T)$. The parameters E_0 and C_1 were determined from the position of the point $T = T_*$ and the value of $n_p(T)$ at high temperatures [27]: (a) $\Delta/E_0 = 0.25$, $E_0 = 0.0831$ eV, $C_1 = 0.146$; (b) $\Delta/E_0 = 0.35$, $E_0 =$ 0.0835 eV, $C_1 = 0.145$. The dislocation densities N_D are the same as the first four values in Fig. 10 (they are calculated on the basis of Ref. [32]).

conditions described in Ref. [27] on the assumption that $S_1 = 1$ is illustrated in Fig. 11 for two values of Δ/E_0 amounting to 0.25 and 0.35. The parameters E_0 and C_1 are selected on the basis of two points of the dependence $n_p(T)$ [the position of $T = T^*$ and the value of $n_p(T)$ at $10^3/T \geqslant 5$]. It follows from Fig. 11 that, as Δ increases, a fan of the $n_p(T)$ curves becomes wider in the vicinity of the point $T = T^*$. However, beginning from $\Delta/E_0 \geqslant 0.25$, the temperature dependences $n_p(T)$ acquire new qualitative details (additional bending), which are not observed in the case of experimental curves. Therefore, an increase in Δ so that it falls in the range $\Delta/E_0 \geqslant 0.25$ is pointless.

The width of the fan of the $n_p(T)$ curves in the vicinity of the point $T = T^*$ is nevertheless still insufficient to account for the experimental situation [26, 27] and the theory should be complicated further by including the Coulomb effects.

3.2.2 The Coulomb interaction between the charges on a dislocation at temperatures in the vicinity of $T = T^*$ can be divided arbitrarily into two components:

$$V_C = V_C^+ + V_C^- \,. \tag{71}$$

The energy V_C^+ corresponds to the variable-sign distribution of the charge along a dislocation when the total charge is zero. It is obvious that $V_C^+ \neq 0$ at the point $T = T^*$ and it can be described by an expression, which represents the form of the Madelung energy of ionic crystals:

$$V_C^+ = \frac{2e^2}{\varepsilon a} f^+ \ln 2 \,, \tag{72}$$

where

$$f^+ = C_1 \left[\exp\left(\frac{E_0 - V_C^+ - F}{T} \right) + 1 \right]^{-1} + S_1 \left[\exp\left(\frac{-E_0 + V_C^+ + F}{T} \right) + 1 \right]^{-1} ,$$

ε is the permittivity, a is the atomic spacing, and F is the chemical potential. The energy V_C^+ reduces the energies of both acceptors and donors of dislocation origin:

$$E_a = E_0 - V_C^+ \,, \quad E_d = E_0 - V_C^+ \,. \tag{72a}$$

We recall, as reported in Section 3.1, that the experimental values of E_a and E_d [26, 27] are similar in the neutral approximation: $E_a \approx E_d \approx E_0$.

The energy V_C^- appears in the absence of compensation of positive and negative charges on a dislocation:

$$f^- = C_1 \left[\exp\left(\frac{E_a^- - F}{T} \right) + 1 \right]^{-1} + S_1 \left[\exp\left(\frac{F - E_d^-}{T} \right) + 1 \right]^{-1} . \tag{73}$$

We can assume that

$$V_C^- = \frac{e^2 f^-}{\varepsilon a} \ln\left(\frac{r_d}{a} f^- \right) , \quad r_d^2 = \frac{\varepsilon T}{4\pi e^2 n_p(T)} \,. \tag{74}$$

The Debye screening means that V_C^- given by expression (74) can be used only in the vicinity of T^*.

If $V_C^- \neq 0$, the energies E_a and E_d are not equal even when they are equal in the neutral model. In fact, if a dislocation as a whole is positively charged, it attracts electrons (the energy E_a decreases) and repels holes (E_d increases). As a result, we can assume that

$$E_a^- = E_0 - V_C^- + \Delta \,, \quad E_d^- = E_0 + V_C^- - \Delta \,. \tag{75}$$

It is obvious that the role of V_C^- becomes greater away from the point $T = T^*$. On the other hand, the presence of V_C^+ has the greatest effect in the vicinity of $T = T^*$. For the sake of generality, the definitions of E_a^- and E_d^- given by expression (75) include $\Delta \neq 0$ taken from expression (70).

The position of the chemical potential $F^\pm$ is described by the following local neutrality equation:

$$N_v(T) \exp\left(\frac{-F^\pm}{T} \right) + \frac{N_D C_1/a}{1 + \exp\left[(-E_d^\pm + F^\pm)/T \right]} = \frac{N_D S_1/a}{1 + \exp\left[(E_a^\pm - F^\pm)/T \right]} + n_a^0 \,, \tag{76}$$

which is valid only in the vicinity of $T = T^*$. Here, n_a^0 is the concentration of point acceptors, $N_v(T)$ is the density of states in the valence band, and the concentration $n_p(T)$ is related to $F^\pm$ by

$$n_p(T) = N_v(T) \exp\left(\frac{-F^\pm}{T} \right) . \tag{77}$$

The solutions of Eqns (76) and (77), in combination with expression (70) under the conditions $V_C^\pm = 0$, gives the results plotted in Fig. 11. Comments on this figure can be found above. Introduction of the energy V_C^+ in the calculations, i.e. the use of the system of equations (76) and (77), together with expressions (72) and (72a), results in a slight renormalisation of E_0 and has practically no effect on the fan of the $n_p(T)$ curves (the effect is less than 10%).

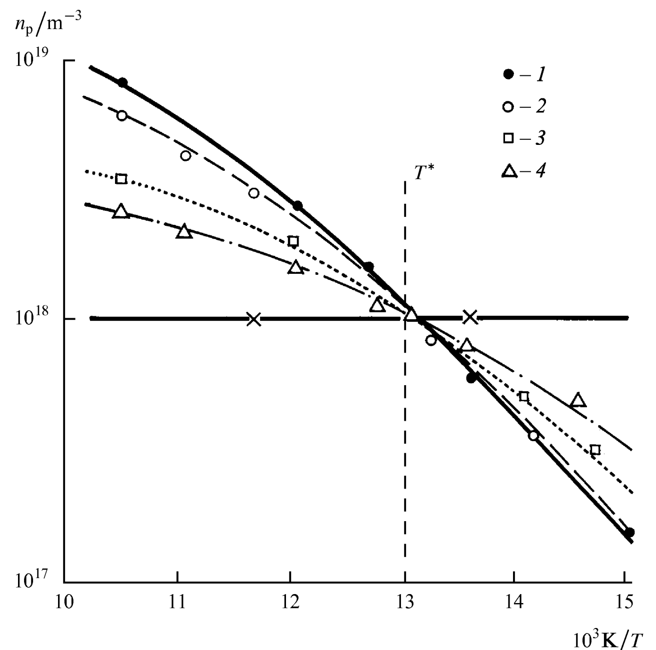

Figure 12. Behaviour of $n_p(T)$ for the case when $\Delta \neq 0$ and the electrons settling at a dislocation experience the Coulomb interaction [32]. Curves *1–4* represent the solution of Eqns (73)–(75) for the experimental values of N_D [27]: (*1*) 3.5×10^{11} m^{-2}; (*2*) 2×10^{11} m^{-2}; (*3*) 7×10^{10} m^{-2}; (*4*) 4.5×10^{10} m^{-2}. The points (×) represent a control sample free of dislocations. Theoretical parameters: $E_0 = 0.0813$ eV, $C_1 = 0.106$, $S_1 = 1$, and $\Delta/E_0 = 0.1624$.

Finally, the behaviour of $n_p(T)$ in the presence of V_C^-, described by expressions (73)–(75), is plotted in Fig. 12 together with the experimental points from Ref. [27] which correspond to different dislocation densities. In this case, the optimal set of the parameters is $E_0 = 0.081$ eV, $C_1 = 0$, and $\Delta/E_0 = 0.16$.

Since the observed properties of $n_p(T)$ reported in Refs [25–27], including the dependence on N_D, can be explained on the basis of the proposed model, it is assumed that $\Delta \neq 0$ and the Coulomb effects that accompany filling of dislocations with electrons are taken into account.

3.3 Origin of an acceptor–donor level

Experiments on single dislocations discussed above indicate that an acceptor–donor level is located above the top of the valence band. However, experiments on the conductivity of a boundary in a germanium bicrystal, which in a sense can be regarded as a periodic system of edge dislocations separated by a distance

$$D = \frac{\boldsymbol{b}}{2\sin(0.5\varphi)}\,, \qquad (78)$$

requires an introduction of a dislocation level below the top of the valence band [34–37]. Here, $\boldsymbol{b}$ is the Burgers vector and φ is the misorientation angle. It might seem that in the opposite case we could not explain the presence of free holes in the vicinity of dislocations as the absolute temperature tends to zero.

Our proposed model of an acceptor–donor level makes it possible to eliminate this qualitative contradiction. This model postulates the deformation origin of such a level. As pointed out above (Section 2), in the vicinity of a single dislocation an electron (hole) experiences a deformation potential which for an edge dislocation considered in the isotropic approximation is

$$V(r, \vartheta) = W\,\frac{1-2\nu}{2\pi(1-\nu)}\,\frac{\boldsymbol{b}}{r}\,\sin\vartheta\,. \qquad (79)$$

Here, W is the deformation interaction constant (for germanium, its value is $W \approx 10$ eV), ν is the Poisson ratio, and ϑ is the angle measured from a dislocation glide plane.

The variable-sign nature of the interaction potential described by expression (79) and the scale of the constant W suggest that at distances r of the order of $\boldsymbol{b}$ an inversion can take place in the electron spectrum when a locally perturbed top of the valence band is found above the perturbed bottom of the conduction band. Development of this hypothesis leads to a number of qualitative consequences:

(a) in an intrinsic semiconductor the electrons at the top of the perturbed valence band begin to undergo transitions to the conduction-band well, creating an electron–hole system;

(b) the Fermi level separating the vacant and occupied states in the band gap of a semiconductor should drop to the top of the perturbed valence band, thus ensuring the appearance of a metallic conduction band of holes distributed along a dislocation, even in the limit $T \to 0$;

(c) the real hole spectrum at the top of the deformed valence band is quantised at right-angles to the dislocation axis and the scale of such quantisation is characterised by the level $E_0 \sim 0.1$ eV above the unperturbed position of the top of the valence band [see the set of expressions (43)];

(d) in a p-type semiconductor the level E_0 at the top of the perturbed valence band begins to play the role of an acceptor–donor level and interacts with point acceptors; this ensures the correct position of this level (above the top of the unperturbed valence band and above the level E_a of point acceptors), which — in principle — resolves the paradox in the interpretation of the properties of a boundary in a bicrystal.

It therefore follows that the deformation interaction of electrons with the elastic field of a dislocation helps to provide a self-consistent description of the experiments on single dislocations and on a chain of such dislocations on the boundary in a bicrystal. However, the mechanism of

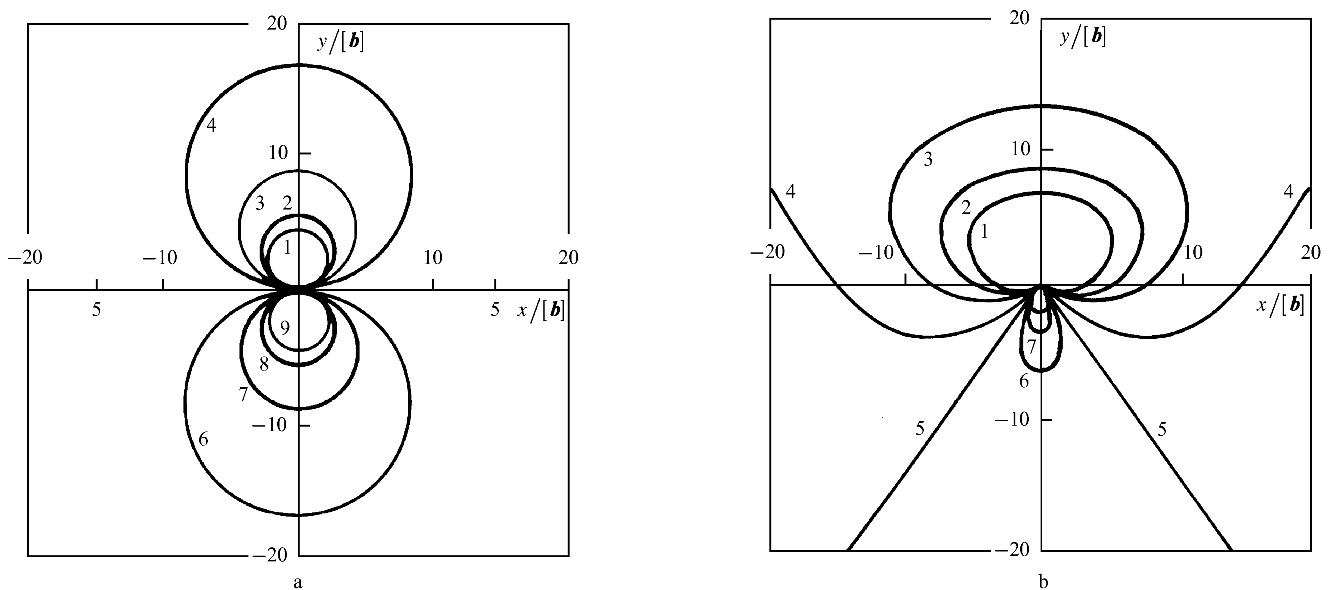

Figure 13. Lines of constant values of the deformation potential of the valence band of germanium, governed by the field of elastic stresses of a 60° dislocation, considered in the hydrostatic approximation (a) and in accordance with expression (82) (b): curves *1–9* correspond to ΔE_v ranging from +0.1 to −0.1 eV in steps of 0.25 eV; $\boldsymbol{b}$ is the Burgers vector of a 60° dislocation.

formation of a two-dimensional hole system along the plane of this boundary is not clear. If, in the isotropic approximation, we consider the distribution of the constant-energy lines of the potential described by expression (79), it is not obvious that an overlap of the hole or electron regions can occur when separate dislocations form a periodic chain (Fig. 13). However, a more rigorous formulation of the problem of the deformation potential given below solves this problem as well [33].

Let us consider a single 60° dislocation. Let us assume specifically that the x axis is directed along the Burgers vector of the edge component of this 60° dislocation, that the z axis is parallel to the direction of the $\langle\bar{0}\bar{1}\bar{1}\rangle$ dislocation line, and the y axis is perpendicular to the glide plane $(\bar{1}\bar{1}\bar{1})$. According to Ref. [38], the strain tensor ε_{ij} of a 60° dislocation can then be expressed in terms of the corresponding strain tensors of a 90° dislocation and of the screw component.

The edge component is characterised by the strains

$$\varepsilon_{11} = \frac{\sqrt{3}\boldsymbol{b}}{8\pi(1-\nu)} \frac{y}{(x^2+y^2)^2} \left[2\nu(x^2+y^2) - y^2 - 3x^2\right] ,$$

$$\varepsilon_{22} = \frac{\sqrt{3}\boldsymbol{b}}{8\pi(1-\nu)} \frac{y}{(x^2+y^2)^2} \left[2\nu(x^2+y^2) - y^2 + x^2\right] , \quad (80)$$

$$\varepsilon_{12} = \varepsilon_{21} = \frac{\sqrt{3}\,\boldsymbol{b}}{8\pi(1-\nu)} \frac{y}{(x^2+y^2)^2} \left(x^2 - y^2\right) .$$

The strains of the screw component are

$$\varepsilon_{13} = \varepsilon_{31} = -\frac{\boldsymbol{b}}{8\pi} \frac{y}{(x^2+y^2)} ,$$

$$\varepsilon_{23} = \varepsilon_{32} = -\frac{\boldsymbol{b}}{8\pi} \frac{y}{(x^2+y^2)} , \quad (81)$$

where $\boldsymbol{b}$ is the Burgers vector of the 60° dislocation and ν is the Poisson ratio.

The deformation potential of the valence band of a cubic crystal is [39]

$$\Delta E_{\rm v} = A\ {\rm Sp}\,\varepsilon_{ij} \pm \Big[0.5B^2\left[(\varepsilon_{11}-\varepsilon_{22})^2 + (\varepsilon_{22}-\varepsilon_{33})^2 + (\varepsilon_{33}-\varepsilon_{11})^2 + d^2(\varepsilon_{12}^2 + \varepsilon_{23}^2 + \varepsilon_{13}^2)\right]\Big]^{1/2} . \quad (82)$$

The plus or minus signs correspond to the splitting of the initially degenerate light-hole and heavy-hole valence subbands of a cubic crystal. The values of the deformation potential constants are given in Refs [39, 40]. For germanium, these constants are $A = -4$ eV, $B = -2.7$ eV, $d = 5$ eV, and $\nu = 0.2$.

The results of calculations of constant-energy lines are presented in Figs 13b and 14. The region $r \leqslant 2\boldsymbol{b}$ is excluded from these calculations because in this region the continuum definitions of ε_{ij} given by the set of expressions (80) diverge. Since the size of the core of a dislocation is $r_0 = (3-5)b$, a calculation carried out on the basis of formulas (80)–(82) is obviously meaningful for $r > r_0$. Fig. 13b shows the structure of the constant-energy lines calculated on the basis of expression (82) for a single dislocation in germanium. It is evident that the region corresponding to a higher concentration of holes occupies a sector with the angle 286°, which is considerably greater than the result obtained in the hydrostatic approximation (Fig. 13a). For $\Delta E_{\rm v} > 0$, the area bounded by a constant-energy line and given by expression (82) is 10 times greater than the corresponding area obtained in the hydrostatic approximation.

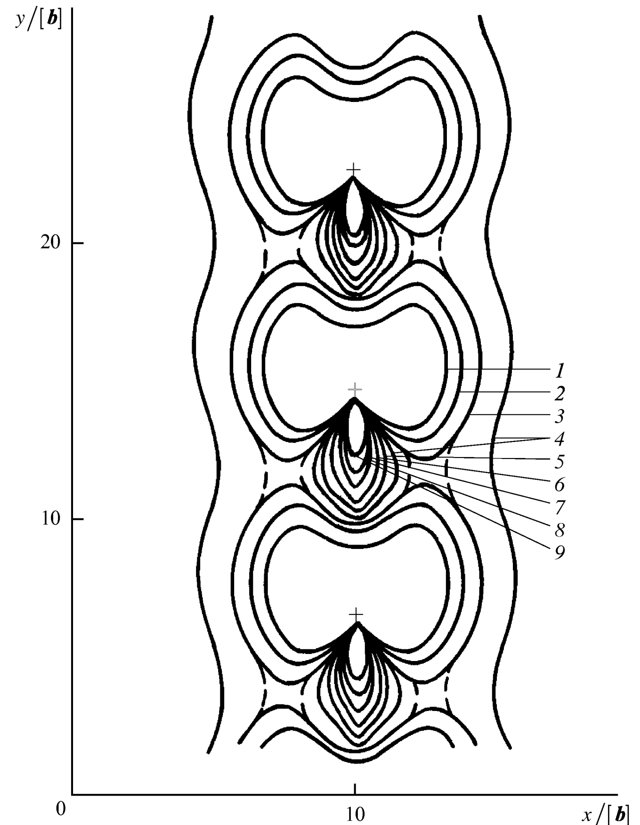

Figure 14. Lines representing constant values of the deformation potential of the valence band of germanium governed by the field of elastic stresses of a boundary in a bicrystal when this boundary consists of a single row of 90° dislocations (the lines are numbered in the same way as in Fig. 13, the dislocation line is directed along [100] and the Burgers vector along [011]).

Let us conclude by considering the results presented in Fig. 14. This figure gives the structure of the constant-energy lines for the valence band of germanium distorted by the field of elastic stresses of the boundary in a bicrystal when this boundary consists of one row of 90° dislocations. The calculations were carried out on the basis of expression (82), selecting the plus sign and the values of the strain tensor given in Refs [39, 40]. A reduction in the distance D between dislocations first creates a pair of constant-energy lines (*4* in Fig. 14) with the minimum positive energy (0.025 eV in our case). Outside these lines the distortions of the valence band fall exponentially. The $\Delta E_{\rm v} = 0$ line for a single dislocation extends to infinity and turns to form a closed loop (line *5* in Fig. 14) localised between dislocations; it compresses the lines with negative energies (lines *6*–*9*). The continuous curves give the solution for $D = 8\boldsymbol{b}$. If $D = 7\boldsymbol{b}$, the 0.05 eV lines transform as shown by the dashed curves and an additional pair of lines appears. For $D = 5\boldsymbol{b}$ a similar transformation affects the 0.075 eV lines. The 0.7 eV lines, corresponding to the depth of a dislocation level relative to the top of the unperturbed valence band, is transformed into a pair of infinite lines for $D = 5.5\boldsymbol{b}$, which — in accordance with formula (78) — corresponds to the misorienta-tion angle 10° of the bicrystal. Experimental investigations [34] show that metallic conduction of the boundary in a germanium bicrystal

appears at $\vartheta \geqslant 8°$. This supports the proposed model of metallic conduction which involves the states of the deformation potential of dislocations.

3.4 Inversion of the type of conduction in plastically deformed n-type semiconductors

In view of the acceptor action of dislocations in germanium and silicon, which manifests itself in a number of ways discussed above, we can assume that a monotonic increase in the dislocation density in an n-type semiconductor should result in inversion of the type of conduction of such a semiconductor, as found also when the concentration of point acceptors in an n-type semiconductor is varied [11]. However, the details of this transition, considered as a function of the relative concentration of acceptors n_a^0/n_d, are very different for point defects and for dislocations. Here, n_a^0 and n_d represent the concentrations of point acceptors and donors. Some aspects of this problem are considered qualitatively below on the basis of Ref. [41]. The structure of the inversion transition is interesting also from the point of view of testing the phenomenological model of dislocation levels, which has proved successful in the description of plastically deformed p-type semiconductors [31, 32].

Specific results relate to the behaviour of the Fermi level in plastically deformed semiconductors considered as a function of the dislocation density N_D at sufficiently low temperatures. The behaviour of the chemical potential F in samples containing point impurities is assumed to be known [11]. Roughly speaking, if the problem is symmetric for electrons and holes, the dependence $F(n_a^0/n_d)$ is a step with its centre at a point $n_a^0 = n_d$ and its width $\varDelta$ is of the order of

$$\varDelta \approx \frac{T}{E_g}\,, \tag{83}$$

where E_g is the band gap.

It is best to start a description of the behaviour of the chemical potential F in a plastically deformed n-type semiconductor, beginning from low dislocation densities N_D, when

$$R^2 \leqslant N_D^{-1}\,. \tag{84}$$

Here, R represents the radius of a Read cylinder around a single charged dislocation. In the geometric approximation $R \gg r_D$ (where r_D is the Debye screening radius, corresponding to the concentration n_d of point donors), the Read radius determines the distance at which the field of a charged dislocation becomes screened.

If inequality (84) is obeyed, the effective equation of neutrality which — as usual — describes the behaviour of the chemical potential, should be written in the following form:

$$N_e \exp\left(\frac{F}{T}\right)\left(1-\frac{V^*}{V}\right)+\frac{N_d f}{a}=n_d\,,\qquad N_e=\frac{2}{\hbar^3}\left(\frac{m_e T}{2\pi}\right)^{3/2}, \tag{85}$$

where V and V^* are the total volume of a crystal and the volume inside the Read cylinders, and m_e is the effective mass of an electron. The first term on the left-hand side of the first equation in the system (85) takes account of the expulsion of electrons from the Read cylinders and the second represents the contribution made to the negative charge density by charged dislocations, each characterised by the filling factor f related to V^* by the first equation in the system (85). The right-hand side of this equation is the concentration of donors assumed to be ionised.

The relationship between f and V^*/V,

$$\frac{V^*}{V}=\frac{N_a f}{a n_d}\,, \tag{85a}$$

shows that the definition of F given by the first equation in the system (85) reduces to its definition in the absence of dislocations [11]:

$$N_e \exp\frac{F}{T}=n_d\,. \tag{86}$$

In other words, dislocations do not influence the behaviour of F, as long as $R^2 < N_D^{-1}$.

Therefore, the solution of the problem of the dislocation-induced inversion of the type of conduction predicts nothing special for the region $n_a/n_d \approx 1$ of the dependence of the chemical potential on the parameter n_a/n_d (in contrast to the case of point centres, where the region $n_a^0/n_d \approx 1$ is critical). In fact, inequality (84) together with $\pi R^2 n_d = f/a$ can be rewritten as

$$R^2 N_d = \frac{f}{\pi}\frac{n_a}{n_d} < 1\,,\qquad n_a=\frac{N_D}{a}\,. \tag{87}$$

Since the maximum value of f for n-type germanium and silicon does not exceed $f \approx 10^{-1}$, it is clear that in the region of $n_a/n_d \approx 1$ an initially n-type semiconductor retains its type of conduction by a large margin, because inequality (87) is not yet violated.

Under the conditions opposite to those specified by inequality (87) (in the $R^2N_D > 1$ range) the dislocations are capable of 'collecting' all the electrons from donors and, therefore, the position of the chemical potential becomes dependent on the dislocation density. This effect is described by us in Ref. [41] with the aid of a cylindrical model which predicts the main properties of inversion in a qualitatively correct manner, with the exception of the critical behaviour of the dislocation density N_D^0 at which the approximation $R^2N_D \geqslant 1$ begins to be valid. The value of N_D^0 depends on details of the distribution of dislocations in a sample and can vary within certain limits of the parameter R^2N_D when its numerical value is ~ 1.

According to the simple cylindrical model, the occupancy factor f of a single dislocation is, as above [see formula (85a)], related to the effective radius R which represents the average distance between dislocations:

$$\pi R^2 n_d = \frac{f}{a}\,. \tag{88}$$

In the absence of free electrons and holes, the concentration of which is assumed to be exponentially small (this is particularly true of silicon), relationship (88) represents the condi-tion ensuring complete neutrality of a crystal.

The position of the chemical potential can be found from the definition of f:

$$f = C_1\left[\exp\left(\frac{+E_1+V_C-F}{T}\right)+1\right]^{-1} + C_2\left[\exp\left(\frac{+E_2+V_C-F}{T}\right)+1\right]^{-1}, \tag{89}$$

$$V_C=\frac{2\pi e^2}{\varepsilon}\,n_d R^2\Big\{2\ln(\pi R^3 n_d)-\big[1-(\pi^2R^6n_d^2)^{-1}\big]\Big\}. \tag{89a}$$

Definition (89) takes account of the structure of dislocation levels deduced from an analysis of the data on the behaviour of dislocations in n-type semiconductors. Moreover, explicit use is made of the advantages of the cylindrical model which yields the fairly simple expression (89a) for V_C.

The critical value of R_0, beginning from which the definition (89) begins to be valid, follows from the requirement that at $R = R_0$ the chemical potential F should occupy a position typical of an n-type semiconductor at $T = 0$ in the absence of dislocations, i.e.

$$F = E_g \ . \tag{90}$$

As a result, the definition of R_0 is

$$\pi R_0^2 n_d a = C_1 \left[\exp\left(\frac{E_1 + V_C(R_0) - E_g}{T} \right) + 1 \right]^{-1} + C_2 \left[\exp\left(\frac{E_2 + V_C(R_0) - E_g}{T} \right) + 1 \right]^{-1} . \tag{91}$$

The behaviour of F in the range $R < R_0$ is plotted in Fig. 15 for $E_1 = 0.42$ eV, $E_2 = 0.62$ eV, $C_2 = 1$, and various values of C_1. Some details of this figure are worth special note. First, the chemical potential F begins to 'sink' into the band gap smoothly and not abruptly, as is true of point impurities. Crossing of the point $R = R_C$ by the level

$$F = 0.5 E_g \ , \tag{92}$$

which corresponds formally to inversion of the type of conduction, is not marked by any singular behaviour. Second, the details of the 'passage' of the chemical potential across the level E_2 are interesting. The jump ΔF that occurs at this level amounts to

$$\Delta F \approx -E_2 + E_1 \tag{93}$$

and the position R_* follows from the estimate

$$\left(\pi R_*^2 n_d a \right)^{-1} \approx C_1 \ . \tag{94}$$

A numerical determination of the value of R_* with the aid of definition (89) carried out for different values of C_1 confirms the dependence $R_*^{-2} \propto C_1$ with the coefficient of proportionality that follows from expression (94). Therefore, in a model of two levels with a limited capacity C_1 the dependence $F(\delta)$, where $\delta = N_D/(n_d a)$, has a characteristic jump at the point of dislocation-induced inversion of the type of conduction and the position of this jump depends on the capacity C_1.

The results obtained can be used in an analysis of the experimental results [28, 42] on dislocation-induced inversion of the type of conduction in silicon. Both investigations were carried out on samples doped with phosphorus donors present in an approximately the same concentration ($n_d = 2 \times 10^{14}$ cm^{-3} in Ref. [28] and $n_d = 2 \times 10^{13}$ cm^{-3} in Ref. [42]). It was found that the type of conduction (revealed by the change in the sign of the Hall coefficient) changed when the dislocation density was varied monotonically. In both cases a jump of the chemical potential was observed on passage through the middle of the band gap. However the positions of this jump δ^* on the δ axis were quite different, as demonstrated in Fig. 15. To the right of the jump, i.e. in the range $\delta > \delta^*$, the results reported in Refs [28] and [42] for $F(\delta)$ show practically no dispersion (this will be used later). In other words, in this range the chemical potential lies at about the same height $E_1 \approx 0.42$ eV above the valence band in both cases.

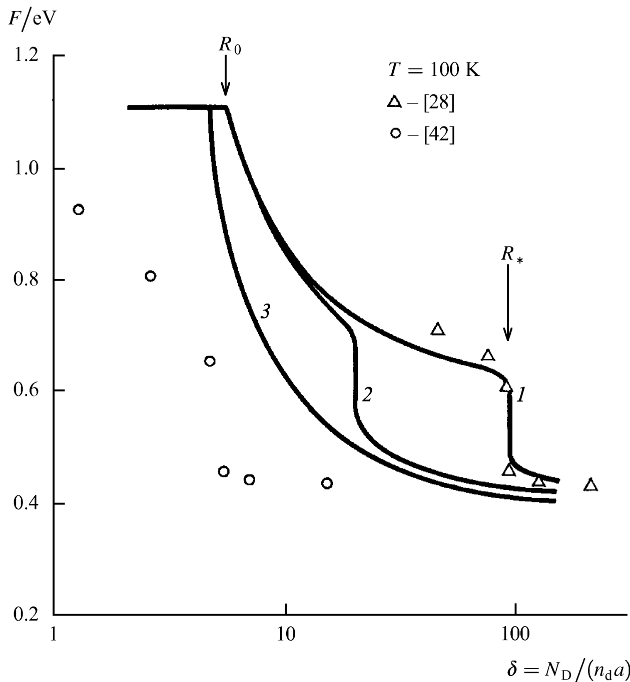

Figure 15. Dependence of the chemical potential F on the dimensionless dislocation density $\delta = N_D/n_d a$, plotted for three values of the parameter C_1: (*1*) $C_1 = 0.01$; (*2*) $C_1 = 0.06$; (*3*) $C_1 = 0.2$. For curves *1* and *3* the constants C_1 were selected so that the calculated positions of the jumps of $F(\delta)$ agreed with the experimental results; curve *2* corresponds to the intermediate case with $C_1 = 0.06$.

The positions of the experimental points in Ref. [42], reproduced in Fig. 15, indicate that they cannot be described by the cylindrical model of the inversion transition developed above. In fact, according to Ref. [42], the chemical potential begins to depend significantly on δ in the range where it should remain constant and independent of the disloca-tion density. Moreover, it is stated in Ref. [42] that there are doubts not only about the cylindrical model of the inversion transition, but also about Read's very idea of localisation of dislocation charges in a narrow tube of radius $C = a/f \ll R$. It follows from the Read model and the data of Ref. [42] that in the range $R > R_0$ the Coulomb energy exceeds the band gap E_g, which should not occur. Attempts to solve this problem led the authors of Ref. [42] to an alternative model in which the dislocation charge is 'smeared out' practically throughout the whole Read cylinder [43].

However, one should point out one experimental detail not very sensitive to the model used in the analysis of the experimental data and found to be practically the same for both series of experiments [28, 42]. As pointed out above, there is practically no dispersion of $F(\delta)$ in the range $\delta > \delta^*$. This behaviour of $F(\delta)$ can be accounted for by the cylindrical model of inversion of the type of conduction in the limiting case $C_1 \ll 1$. However, if C_1 lies near the value $C_1 \approx 0.2$, where the jump of F reported in Ref. [42] is located, it then follows from Fig. 15 that a strong dispersion of $F(\delta)$ is unavoidable, but this is not observed experimentally.

Therefore, the absence of significant dispersion of $F(\delta)$ in the range $\delta > \delta^*$ reported in Ref. [42] indicates, in our

view, that the real value of C_1 is $C_1 \ll 1$. In other words, the dislocation densities found in Ref. [42] from the edge pits are somewhat underestimated compared with the real values. On the other hand, the dislocation densities are probably overestimated in Ref. [28] (they were obtained by the ESR method). Therefore, the exact value of the capacitance C_1, which is of the order of $C_1 = 0.01$ (curve *1* in Fig. 15), may be found more accurately in the subsequent experiments. However, it is clear that the constant C_1 would be quite small ($C_1 \ll 0.1$).

3.5 Inversion of the type of conduction in germanium

There is no detailed experimental information on the behaviour of the chemical potential of germanium in the vicinity of its jump, but detailed investigations have been made in the region where $R < R_*$ and $R \leqslant R_0$.

A quantitative description of the vicinity of the jump ΔF and of the behaviour of the effective density of holes $n_p(T)$ has to allow for the influence of holes, the role of which is quite significant, particularly at higher temperatures. Moreover, the density $n_p(T)$ is an observable quantity, which can be used to follow the evolution of inversion in the p-type range.

The finite concentration of holes modifies, in the calculations relating to the behaviour of F, expression (88) which now becomes

$$\pi R^2 n_d + 2\pi \int_{r_0}^{R} n_p(r)\, r\, dr = \frac{f}{a}, \qquad (95)$$

where

$$n_p(r) = n_p^0 \exp\frac{e\varphi}{T}, \qquad (96a)$$

$$\Delta\varphi = 4\pi e \varepsilon^{-1}\left[n_d + n_p(r)\right], \qquad (96b)$$

$$\varphi'|_{r=R} = 0, \quad \varphi|_{r=R} = 0. \qquad (97)$$

Here, $n_p(r)$ is the concentration of holes in the vicinity of a dislocation and ε is the permittivity of the semiconductor. The boundary conditions (97) for the electric potential $\varphi(r)$ are satisfied if we neglect the contribution of free electrons to the overall neutrality of a crystal.

The values of $n_p(R)$ calculated in Ref. [44] with the aid of expressions (89), (95)–(97) are plotted in Fig. 16 alongside the experimental results [27].

Interesting results are also plotted in Fig. 9 of Ref. [24], where several effects worth attention can be observed simultaneously.

First, we can clearly see a 'fork' in the temperature dependences $\sigma_{\parallel}(T)$ and $\sigma\perp(T)$. The appearance of this fork is discussed above in comments following expression (54).

Second, it is possible to observe a gradual 'sinking' of the chemical potential of germanium in the lower part of the band gap (left-hand sides of curves *2–4*). We recall that in the case of silicon this part of the temperature dependence of the chemical potential has not yet been determined experimentally, as can be seen in Fig. 15 where the upper part of the dependence $F(N_D)$ has practically no experimental points.

Third, we can show that in the range $T < T_0$ the transverse motion is hindered by an additional potential barrier whose height increases smoothly with increase in the dislocation density.

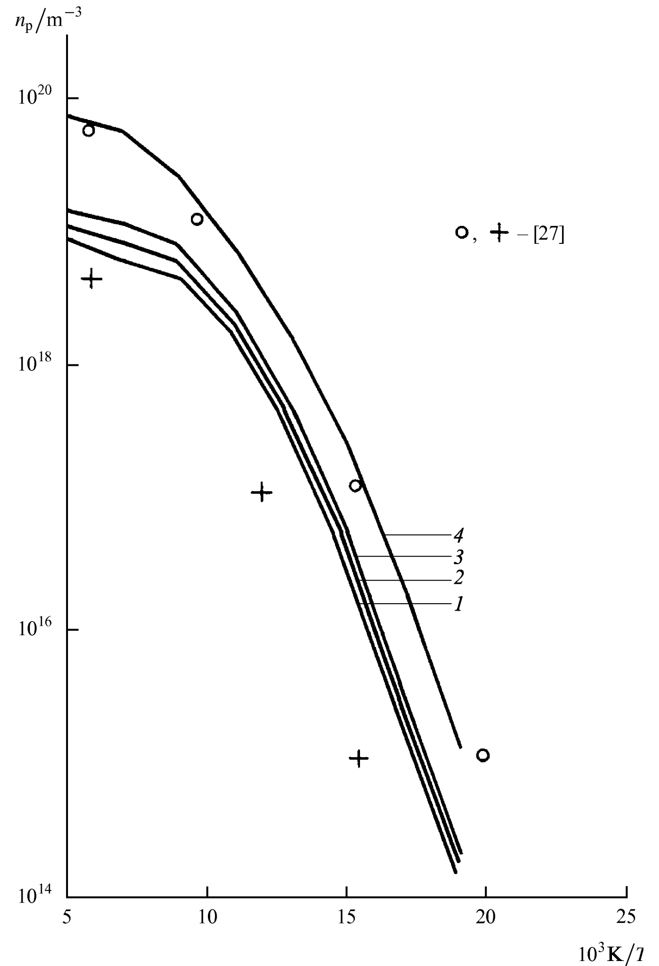

Figure 16. Concentration of holes in plastically deformed n-type germanium calculated on the basis of a model with two electron levels. The parameters used in the calculations were: $E_1 = 0.11$ eV, $C_1 = 0.1$, $E_2 = 0.28$ eV, $n_d = 5 \times 10^{11}$ cm^{-3}. The dislocation densities N_D were: (*1*) 5×10^6 cm^{-2}; (*2*) 4×10^6 cm^{-2}; (*3*) 5.5×10^6 cm^{-2}; (*4*) 3×10^7 cm^{-2}. The parameters of this spectrum were selected to ensure the best agreement of curve *4* with the experimental data (o) taken from Ref. [27] (the calculations were reported in Ref. [44]).

4. Current – voltage characteristics of a sample with charged dislocations

One of the reasons for the appearance of potential barriers hindering the passage of an electric current in semiconductors may be a system of oriented dislocations of sufficient density. Such a system may appear, for example, at low-angle grain boundaries or at boundaries in bicrystals [34–36, 45] when the Read cylinders of adjacent charged dislocations overlap. Another form of a dislocation barrier is encountered in the problem of electrostatic properties of semi-conductors containing a set of charged dislocations all oriented in the same direction. The possibility of formation of an array of charged dislocations of this type has been demonstrated in a number of experiments [24, 46]. The degree of orientation of these dislocations reported in these papers reached 1 : 10. Obviously, an increase in the dislocation density or cooling of a sample will result in the overlap of the Read cylinders of the adjacent dislocations giving rise to an infinite cluster dissecting the whole sample. The unavoidable appearance

of such a cluster follows from general propositions of the modern theory of percolation [47]. From our point of view such a cluster is a barrier of dislocation origin and its appearance considerably affects the electric properties of a semiconductor.

Dislocation barriers have a characteristic feature in the form of saddle points, and the flow of free electrons overcoming a barrier occurs mainly at these points. It is therefore necessary to develop a special theory of the current – voltage characteristics for the flow of an electric current across a dislocation barrier.

In this section we shall present a general formalism which makes it possible to describe, in the diffusion approximation, the properties of barriers with arbitrarily deep saddle points. We shall derive the current – voltage and capacitance–voltage characteristics under ohmic conditions for a semiconductor containing a dislocation barrier; this will be done in the limiting cases of a strong or weak overlap of the Read cylinders. We shall discuss the role of random fluctuations of the barrier profile.

4.1 Current – voltage characteristic of a barrier with saddle points

Calculation of the current – voltage characteristic representing the flow of an electric current across a potential barrier reduces to solution of the equation of continuity $\mathrm{div}\boldsymbol{j} = 0$ in the vicinity of this barrier and subject to certain boundary conditions at the barrier edges. These conditions take account of an external potential difference. This procedure has been developed in detail for one-dimensional barriers and it can be applied also to barriers with saddle points.

4.1.1 Let us consider the specific case when charged dislocations are distributed periodically along the y axis and the period is d. The x axis is normal to the barrier plane. In the diffusion approximation the current density is given by the familiar expression:

$$j_1 = -\sum \mu_{ik}\left(T\frac{\partial n}{\partial x_k} + en\frac{\partial \varphi}{\partial x_k}\right), \tag{98}$$

where μ_{ik} are elements of the matrix

$$\mu_{ik} = \mu\delta_{ik}, \quad i = 1, 2; \quad k = 1, 2, \tag{99}$$

where $x_1 \equiv x$, $x_2 \equiv y$; the barrier is elongated along the y axis; μ is the electron mobility; T is the absolute temperature; n is the electron concentration; φ is the electrostatic potential.

The solution of the equation $\mathrm{div}\boldsymbol{j} = 0$ with j given by expression (98) can be found conveniently in the vicinity of a saddle point if Langer's recommendations are followed [48]. We will therefore expand the potential $\varphi(x, y)$ near a saddle point as a Taylor series:

$$\varphi(x, y) \approx \varphi_s + 0.5(\lambda_2 y^2 - \lambda_1 x^2), \quad \lambda_i = \left.\frac{\partial^2\varphi}{\partial x^2}\right|x_i \to x_s, \tag{100}$$

where φ_s and λ_i are the potential and its curvature at a saddle point.

Factorisation of the potential $\varphi(x, y)$ is accompanied, as indicated in Ref. [48], by vanishing of the y component of the total current so that the dependence of the electron density on the coordinate y is of the equilibrium (Boltzmann) nature:

$$n(x, y) = \sigma(x)\exp\left[-\frac{e\varphi(x, y)}{T}\right], \tag{101}$$

where $\sigma(x)$ is an arbitrary function of x. The x component of the current can be obtained from expression (98) and from $n(x, y)$ given by the above expression:

$$j_x(y) = -\mu T\frac{\partial\sigma}{\partial x}\exp\left(-\frac{e\varphi_s + 0.5e\lambda_2 y^2}{T}\right), \tag{102}$$

on condition that

$$\frac{\partial\sigma}{\partial x} = \frac{j_0}{\mu T}\exp\left(-\frac{e\lambda_1 x^2}{2T}\right) \tag{103}$$

or

$$\sigma(x) = -\frac{j_0}{\mu T}\int_{-\infty}^{x}\exp\left(-\frac{e\lambda_1 x^2}{2T}\right)\mathrm{d}x + C. \tag{103a}$$

The constants j_0 and C in the above expression can be found by applying the boundary conditions for $n(x, y)$ at the barrier edges. It is assumed that far from a saddle point the potential $\varphi(x, y)$ becomes one-dimensional and depends only on the coordinate x. In other words,

$$\begin{aligned} &n = n_d, \quad \varphi = 0 \quad \text{for} \quad x \to -\infty, \\ &n = n_d, \quad \varphi = -V \quad \text{for} \quad x \to +\infty, \end{aligned} \tag{104}$$

where n_d is the donor concentration and V is the external potential applied to a barrier. It follows from the definitions of n and $\sigma(x)$, given by expressions (101) and (103a), and from the above conditions that

$$C = n_d, \ j_0 = \mu T n_d\left[1 - \exp\left(-\frac{eV}{T}\right)\right]\left(\frac{\lambda_1}{2\pi T}\right)^{1/2}. \tag{105}$$

The average current per one period of the investigated dislocation chain is [49, 50]:

$$\begin{aligned} j_x &= \frac{1}{D}\int_{-\infty}^{+\infty} j_x(y)\,\mathrm{d}y \\ &= \mu T n_d d^{-1}\left[1 - \exp\left(-\frac{eV}{T}\right)\right]\exp\left(-\frac{e\varphi_s}{T}\right)\left(\frac{\lambda_1}{\lambda_2}\right)^{1/2} \\ &\approx |eV < T| \approx \frac{e\mu n_d V}{D}\left(\frac{\lambda_1}{\lambda_2}\right)^{1/2}\exp\left(-\frac{e\varphi_s}{T}\right), \end{aligned} \tag{106}$$

where $j_x(y)$ is given by expression (102). Therefore, the problem of calculation of the barrier conductivity reduces to determination of the values of φ_s and λ_i. If there is a scatter of the values of D and φ_s, then expression (106) should be averaged over all possible values of D and φ_s with the suitable weights. The problem will be discussed in detail later.

4.1.2 The results presented above are quite rigorous in the range $(e\varphi_{max} - e\varphi_s)/T \gg 1$. However, if $(e\varphi_{max} - e\varphi_s)/T < 1$, the Langer approximation, in particular the expansion of $\varphi(x, y)$ described by expression (100), loses its precision and this makes it difficult to investigate the limiting case of the current – voltage characteristic for a one-dimensional barrier. Consequently, it is sensible to consider one more way of solving the problem of the current – voltage characteristic for a dislocation barrier in the case when $(e\varphi_{max} - e\varphi_s)/T < 1$.

Let us assume that dislocations are distributed periodically (period D) along the crest of a barrier. Let us expand all the functions of interest to us as Fourier series:

$$n(x, y) = \sum n_k(x)\cos(k\omega y)\,, \quad \varphi = \sum \varphi_k \cos(k\omega y)\,,$$

$$j_x = -\sum j_{xk}(x)\cos(k\omega y)\,, \; j_y = -\sum j_{yk}(x)\sin(k\omega y)\,,$$

$$\omega = \frac{2\pi}{D} \tag{107}$$

and let us try to satisfy the equation $\mathrm{div}\boldsymbol{j} = 0$ approximately by separating the harmonics in the nonlinear term $n(\partial\varphi/\partial x_k)$ in the general expression (98) for the current density.

In the zeroth approximation, we have

$$\frac{\partial j_{x0}}{\partial x} = 0$$

or

$$j_{x0} = \mathrm{const} = -T\mu n_0' - e\mu(n_0\varphi_0' + 0.5n_1\varphi_1')\,, \quad n' = \frac{\mathrm{d}n}{\mathrm{d}x}\,. \tag{108}$$

In the zeroth approximation the contribution of the higher harmonics is ignored. The influence of the periodic relief of the barrier is related to the presence in expression (108) of a term corresponding to $n_1\varphi_1$.

In the first approximation, we find that

$$\frac{\partial j_{x1}}{\partial x} + \frac{\partial j_{y1}}{\partial y} = 0\,, \tag{109}$$

$$\varphi_1'' - \omega^2\varphi_1 = -\frac{4\pi e n_{s1}}{\varepsilon}\,, \tag{110}$$

where

$$\varphi_1|_{\pm\infty} \to 0\,, \quad \varphi'|_{x\to+0} - \varphi_1'|_{x\to-0} = -\frac{4\pi e n_{s1}}{\varepsilon}\,.$$

Here, n_{s1} is the Fourier component of the surface charge density

$$n_s(y) = \sum n_{sk}\cos(k\omega y)\,. \tag{111}$$

The zero boundary conditions for φ_1 are valid at large distances as long as $L \gg d$, which is assumed to be obeyed.

Eqn (109), written out explicitly to within terms of the order of n_{s1} and φ_1, and the boundary conditions for this equation are:

$$-Tn_1''(x) - en_{s1}'\varphi_0' - en_{s1}\varphi_0'' - en_0'\varphi_1'$$
$$-en_0\varphi_1'' + \omega^2(Tn_{s1} + en_0\varphi_1) = 0\,, \tag{112}$$

$$n_{s1}\Big|_{x\to\pm\infty} \to 0\,, \quad n_{s1}\Big|_{x=0} = \frac{e\varphi_1}{T}\,n_0\Big|_{x=0}\,. \tag{113}$$

The second of the above boundary conditions is equivalent to the requirement $j_{y1}(0, y) = 0$, which should be satisfied at the crest of the barrier.

If the total current across the barrier is zero, the condition $j_{y1} = 0$ is obeyed identically and it reduces to the following requirement for all values of x:

$$n_{s1}(x) = \frac{e\varphi_1(x)}{T}\,n_0(x)\,. \tag{114}$$

Moreover, j_{x1} also vanishes and the equality $j_{x1} = 0$ follows automatically if relationships (108)–(112) are obeyed.

We shall omit details of the method used to solve the system of equations (107)–(114) and give the first approximation for the current–voltage characteristic:

$$j_{x0} = \frac{e\mu n_d V}{\displaystyle\int_{-L}^{+L} \exp\left[e\varphi_0(x)/T - e^2\varphi_1^2(x)/4T^2\right]\mathrm{d}x}\,, \tag{115}$$

where

$$\varphi_1(x) = -\frac{2\pi e n_{s1}}{\varepsilon\omega}\exp\left(-\omega|x|\right)\,. \tag{116}$$

In the limit $\varphi_1 \to 0$ the characteristic described by expression (115) reduces to the familiar expression for the current–voltage characteristic of a one-dimensional barrier.

4.2 Parameters of saddle points

Calculation of the parameters of saddle points of a dislocation barrier is a fairly difficult self-consistent problem. The situation simplifies in the limiting cases of a strong ($D \ll R$) or weak ($D \leqslant R$) overlap of the Read cylinders of radius R when analytic calculations can be completed. We shall consider each of these limiting cases separately.

4.2.1 Strong overlap. We shall omit the details of the calculations [49, 50] and give only a summary of the main results:

$$\varphi(x, y) = 2\pi L^2 e n_d \varepsilon^{-1}\left(1 - \frac{|x|}{L}\right)^2$$
$$+ 2den_d L\varepsilon^{-1}\left(\frac{2\pi|x|}{D} - \ln\left[2\left(\cosh\frac{2\pi x}{D} - \cos\frac{2\pi y}{D}\right)\right]\right)\,, \tag{117}$$

where

$$L = \frac{n_s}{2n_d}\,, \quad n_s = \frac{f}{Da}\,.$$

Here, ε is the permittivity of the investigated crystal, n_d is the volume concentration of donors, f is the occupancy factor of a single dislocation, and a is the atomic spacing.

The value of φ at certain characteristic points is

$$\varphi_s = \varphi_0\left(1 - \frac{2D}{L}\ln(2)\right)\,, \tag{118}$$

$$\varphi_{\max} = \varphi_0\left(1 + \frac{2D}{L}\ln\frac{D}{2\pi c}\right)\,, \tag{118a}$$

where

$$\varphi_0 = 2\pi e n_d L^2\varepsilon^{-1}\,, \quad c = \frac{a}{f}\,, \quad \frac{D}{2\pi c} \gg 1\,.$$

The quantities φ_s, $\varphi_{\max}$, and φ_0 occur in the definition of significant characteristics of a barrier. For example, the quantity φ_s occurs in the exponential function used to describe the current-voltage characteristic. The potential $\varphi_{\max}$ is needed in the calculation of the occupancy factor f of a charge dislocation in a barrier, found from the relationship

$$-E_D + V_C = F\,,$$

where $V_C = e\varphi_{max}$ is the Coulomb energy of an electron at a dislocation, E_D is the position of a dislocation level, and F is the Fermi level. Finally, the potential φ_0 occurs in the definition of the barrier capacitance C_b:

$$C_b = \frac{Q}{\varphi_0} = \frac{\varepsilon S}{2\pi L} , \qquad (119)$$

where S is the contact area and Q is the total charge.

It is worth noting that all three characteristics φ_s, φ_{max}, and φ_0 are identical for a one-dimensional barrier. In fact, if in expression (118) we go to the limit $(D/L) \to 0$, we find that $\varphi_s = \varphi_{max} = \varphi_0$.

4.2.2 Weak overlap. A rough idea of the properties of a saddle point of two weakly overlapping Read cylinders can be obtained from a simple geometric representation (Fig. 17) with the parameters of the problem corresponding to single Read cylinders. Let us assume that h is the degree of overlap. The chord $2b_0$ along which two cylinders are in contact is related to h by

$$b_0 \approx (2Rh)^{1/2} , \quad R \gg b_0 \gg h \gg r_D , \qquad (120)$$

where R is the Read cylinder radius and $\pi R^2 n_d = f/a$.

The distribution of the potential φ in the contact zone can be found by combining two cylindrically symmetric solutions for the potential of a single charged dislocation $\varphi_0(x, y)$ when the overlap of these cylinders is h:

$$\tilde{\varphi}(x,y) = \varphi_0(x, y + R - h) + \varphi_0(x, y - R + h) , \qquad (121)$$

$$\varphi_0(x,y) = \frac{ef}{\varepsilon a}\left[2\ln\frac{R}{(x^2+y^2)^{1/2}} - \left(1 - \frac{x^2+y^2}{R^2}\right)\right] . \qquad (121a)$$

The coordinates of the saddle points are $x = y = 0$. We then have

$$\tilde{\varphi}_s = \frac{4\pi e n_d h^2}{\varepsilon} , \quad \tilde{\varphi}''_x = -\frac{8\pi e n_d h}{\varepsilon R} ,$$
$$\tilde{\varphi}''_y = 8\pi e n_d \frac{1 + h/R}{\varepsilon} . \qquad (122)$$

However, it should be pointed out that the formula for $\tilde{\varphi}_s$ in expression (122) is not the final one. An overlap between the Read cylinders means that the segments of these cylinders within the contact zone contain no free electrons and, therefore, they do not participate in neutralisation of the fields of charged dislocation lines. The resultant free-electron deficit should be compensated by the regions which lie outside the contact and have no free electrons and, therefore, do not participate in neutralisation of the fields of charged dislocation lines. This can be taken into account within the framework of the adopted approximation of a superposition of two cylindrically symmetric solutions described by expression (121) by placing an additional charge σ_- in the contact zone and an opposite charge σ_+ outside the contact. Obviously, the charge σ_+ should be located as close as possible to the contact zone.

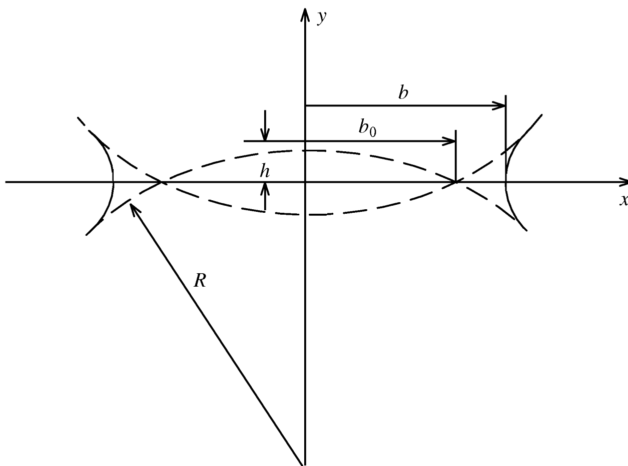

Figure 17. Contact of two Read cylinders with a small overlap. The continuous curves represent the real boundaries of these cylinders.

If we assume that the additional charges are of the surface type, then

$$\sigma(x) = \sigma\left(1 - \frac{x^2}{b_0^2}\right) , \quad \sigma = e n_d h < 0 , \qquad (123)$$

$$\sigma(x) = \begin{cases} < 0 , & 0 \leqslant x \leqslant b_0 , \\ > 0 , & b_0 \leqslant x < b , \end{cases} \qquad (123a)$$

The quantity b is found from the condition

$$\int_{-b}^{+b} \sigma(y)\,dy = 0 \qquad (124)$$

and is given by

$$b = \sqrt{3}\, b_0 . \qquad (124a)$$

The harmonic potential $\varphi^{(1)}$, corresponding to the charge distribution given by expression (123) calculated at a saddle point, is

$$\varphi_s^{(1)} = \frac{2b_0 b\sigma}{\varepsilon(b - b_0)} \ln\frac{b}{b_0} \simeq \frac{3.7\sigma}{\varepsilon}(hR)^{1/2} . \qquad (125)$$

Therefore, the potential at a saddle point for a weak overlap of the Read cylinders is

$$\varphi_s = \frac{\sigma\left[4\pi h + 3.7(hR)^{1/2}\right]}{\varepsilon} . \qquad (126)$$

The distribution of the potential in the contact zone in the case when there is a potential difference between the edges of a barrier deserves separate discussion. The qualitative features of such a problem can be formulated explicitly:

$$\Delta\psi = 0 ,$$
$$\psi(r, \vartheta) = \begin{cases} V & \text{for } \alpha \leqslant \vartheta \leqslant \pi - \alpha , \\ -V & \text{for } \pi + \alpha \leqslant \vartheta \leqslant 2\pi - \alpha , \end{cases} \quad \alpha = \frac{b}{R} . \qquad (127)$$

The distribution in this case is

$$\psi(r, \vartheta) = \frac{2V}{\pi} \arctan\frac{2Rr\sin\vartheta}{R^2 - r^2} . \qquad (128)$$

Expression (128) is derived from the relationship

$$\sum A^{2n+1} \frac{\sin(2n+1)\vartheta}{2n+1} = 0.5 \arctan\frac{2A\sin\vartheta}{1 - A^2} . \qquad (129)$$

The barrier capacitance is

$$C_b = \frac{Q}{V} = D_3 D_2 V^{-1} \int \sigma(\vartheta)\,d\vartheta = \frac{\varepsilon D_2 D_3}{\pi R} \ln\frac{2R}{b} , \qquad (130)$$

where D_2 and D_3 are the barrier dimensions along the y and z axes.

The definition of C_b given by expression (130) together with expression (106) for the current density j_x,

$$j_x = \frac{e\mu n_d V}{D}\left(\frac{h}{R}\right)^{1/2}\exp\left(-\frac{e\varphi_s}{T}\right), \tag{131}$$

which takes account explicitly of the values φ_s and $(\lambda_1/\lambda_2)^{1/2}$ given by expressions (126) and (122), complete the task of description of the properties of a barrier with a weak overlap of the Read cylinders ($D = R - h$, $h \ll R$).

4.3 Influence of random fluctuations of the barrier profile

We shall now consider deep saddles when on the average we have $(e\varphi_{\max} - e\varphi_s)/T \gg 1$. The total conductivity of a barrier then consists of the conductivities of the separate saddle points (which represent conductors connected in parallel):

$$I = \sum_{e}\langle j_x(h_e)\rangle . \tag{132}$$

Introduction of the probability $\omega(h_e)$ of the appearance of a given value h_e and assumption that this probability is Gaussian makes it possible to rewrite expression (132) as follows:

$$\langle j_x\rangle = \frac{I}{D_2} = \int_{-\infty}^{+\infty}\omega(\delta_e) j_x(h_e)\,\mathrm{d}\delta_e , \tag{133}$$

where $\delta_e = D_e - D$, $h_e = h + \delta_e$, $\omega(\delta_e) = \sqrt{2/\pi}\,\Delta^{-1}\times \exp(-\delta_e^2/2\Delta^2)$, Δ is the variance of the distribution of δ_e, and $j_x(h_e)$ is obtained from expressions (131) and (126). If we now assume that $\delta \ll D$, $h \ll D$, we find from expression (133) that:

$$\langle j_x\rangle = j_x(\bar h)\sqrt{\frac{2}{\pi}}\,\Delta^{-1}\int_{-\infty}^{+\infty}\exp\left(-\frac{\delta_e^2}{2\Delta^2} - p\delta_e\right)\mathrm{d}\delta_e$$

$$= j_x(h)\exp(0.5p^2\Delta^2), \quad p = \frac{3.7e^2 n_d}{\varepsilon T}\,\frac{3}{2}\sqrt{hD} . \tag{134}$$

Therefore, fluctuations of the barrier profile, characterised by the variance Δ, give rise to an additional exponential factor in the definition of $\langle j_x\rangle$, which makes it possible to detect quite simply the influence on fluctuations of the current–voltage characteristic.

We shall complete this theoretical introduction by considering an experimental method for the investigating barriers with possible saddle points. Such an investigation can be carried out if the current–voltage and the capacitance–voltage characteristics depend on temperature and on the potential difference V applied to the barrier edges.

The first qualitative question, whether a barrier is of quantum or classical nature, is answered by an analysis of the temperature dependence of the current–voltage characteristic plotted using the coordinates $\ln\langle j\rangle$ and T^{-1}. Rectification of the characteristics in terms of these coordinates indicates activated-type behaviour of the current, i.e. classical behaviour, and makes it possible to determine the barrier activation energy.

Comparison of the barrier heights deduced from the temperature dependence of the current–voltage characteristic and from determination of the capacitance–voltage characteristic in the ohmic region should answer the question whether there are saddle points on a barrier or is the barrier one-dimensional. A one-dimensional barrier has only one characteristic height [see expression (118)]. If saddle points are present, the information which can be deduced from experimental determination of the current–voltage and capacitance–voltage characteristics can give information on qualitatively different details of the investigated barrier. We must bear in mind that in the ohmic range the barrier capacitance is not always given by the simple expression (119).

An additional characteristic of a barrier with deep saddle points is the behaviour of the current–voltage characteristic in the region where the dependence on V is nonlinear. An increase in V across a one-dimensional barrier results in a characteristic plateau of the current–voltage characteristic, which appears because a finite current across a barrier increases the filling factor of bound electron states that determine the barrier height, i.e. such a current stimulates barrier growth. The density of the current flowing across a barrier with deep saddle points is concentrated mainly far from charged dislocations. This is indicated indirectly by the distribution of the perturbing potential $\psi(r, \vartheta)$ described by expression (128), which vanishes on the axes of the Read cylinders (i.e. at the point $r = 0$). As a result, the current–voltage characteristic for a barrier with deep saddle points should not have a definite flat region linking the ohmic region and the breakdown part of the characteristic.

The last interesting detail we should mention is detection of fluctuations of the dislocation barrier profile. These fluctuations can be deduced from an analysis of the ohmic part of the temperature dependence of the current–voltage characteristic considered in terms of the coordinates $\ln\langle j\rangle$, T^{-1}. According to expression (134), if $\Delta \neq 0$, then considerable deviations from linearity (associated with the presence of a term proportional to T^{-2} in the argument of the exponential function) should occur in the $\ln\langle j\rangle$ plane.

Not all the experiments described above have been carried out so far. However, those that have been published support the theoretical predictions.

4.4 Experiments on dislocation barriers

4.4.1 In those cases when the postulated deviation γ from a one-dimensional barrier, which may be described by formula (135) given below, is not too large, a convenient method for detecting this involves simultaneous investigation of the barrier current–voltage and capacitance–voltage characteristics. The former characteristic gives information on the height of the barrier saddle points $V_{\min}$ and the capacitance–voltage characteristic provides the average barrier height $\bar V$. In the presence of saddle points, we have $V_{\min} < \bar V$. The ratio

$$\frac{V_{\min}}{\bar V} = \gamma \leqslant 1 \tag{135}$$

can be used as a measure of departure of a barrier from the one-dimensional approximation. In the one-dimensional case, we have $\gamma \to 1$.

It should be pointed out that inequality (135) is a necessary requirement which follows from an analysis of the properties of a barrier with saddle points. Therefore, when this inequality is satisfied, it implies self-consistency of the experimental data on the current–voltage and capacitance–voltage characteristics of this barrier.

Let us now discuss, on the basis of Ref. [51], the experimental results reported in Ref. [45] on the cur-

rent – voltage and capacitance – voltage characteristics of a dislocation wall formed deliberately in n-type silicon in which the donor concentration is $n_{\mathrm{d}} \sim 10^{14}\ \mathrm{cm}^{-3}$. The average distance D between dislocations in this wall is less than the size L of the region of screening of the dislocation charge by free electrons, so that the overlap of the adjacent Read cylinders, representing the screening properties of the medium with a single charged dislocation should be sufficiently strong and the parameter γ of expression (135) should be close to unity.

In principle, information on the current – voltage and capacitance – voltage characteristics in the range which is linear in respect of the perturbing potential V should be sufficient to find the properties of the parameter γ. However, the results reported in Ref. [45] have a number of special features which make it necessary to use a more complex procedure. First, the current – voltage characteristic reported in Ref. [45] has an ohmic region followed by the above-mentioned plateau of the dependence $I(V)$ (I is the current across the barrier) in the range $eV/T \sim 10 \gg 1$. On the other hand, various theories of the current – voltage characteristics [52 – 55], which postulate that the barrier is purely electrostatic, predict the appearance of this plateau for values $eV/T \gg 1$ (Fig. 18, where the current – voltage characteristic is plotted for the one-dimensional variant employing the diffusion approximation and the parameters taken from Ref. [45]). Obviously, some technical errors were made in plotting Fig. 1 in Ref. [45]: these errors are revealed only if the characteristic is plotted for a wide range of the parameter eV/T: $0 \leqslant eV/T \leqslant 10$. Second, the properties of the capacitance – voltage characteristic in the linear regime can be determined only if precise information is available on the barrier geometry, which again is not very satisfactory in Ref. [45]. Therefore, in the case of the latter

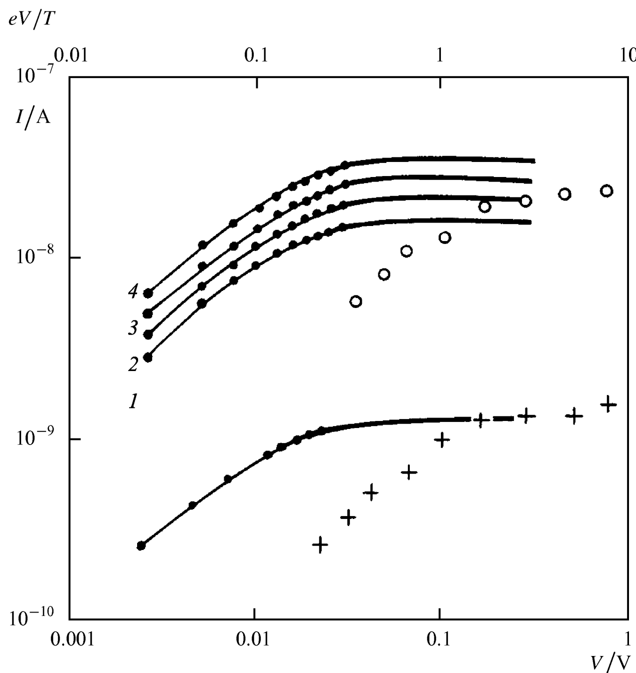

Figure 18. Dependence $I(V)$ at $T = 264$ K and $T = 296$ K, plotted using the coordinates employed in Ref. [45]. Curves *1 – 4* correspond to different values of E_{D}: 0.55, 0.60, 0.65, and 0.70 eV, respectively. The top abscissa gives the values of eV divided by T.

characteristic one has to consider also the nonlinear range where the information about $\bar{V}$ can be obtained from the relative values insensitive to the exact barrier geometry.

Specific calculations were carried out in the diffusion approximation [51] with the aid of the one-dimensional formulas [see also expression (115)], investigated in detail by many authors beginning with Taylor et al. [52]:

$$j = \frac{\mu T n_{\mathrm{d}} \left[1 - \exp(-eV/T)\right]}{\displaystyle\int_{-L_1}^{L_2} \exp(e\varphi/T)\,\mathrm{d}x}\,, \tag{136}$$

$$\varphi(x) = \begin{cases} \dfrac{2\pi e n_{\mathrm{d}} (x - L_2)^2}{\varepsilon} - V\,, & x > 0\,; \\ \dfrac{2\pi e n_{\mathrm{d}} (x + L_1)^2}{\varepsilon}\,, & x < 0\,, \end{cases}$$

where

$$L_{1,2} = \frac{n_{\mathrm{s}}}{2n_{\mathrm{d}}} \pm \frac{\varepsilon V}{4\pi e n_{\mathrm{s}}}\,, \quad n_{\mathrm{s}} = \frac{f}{aD}\,, \quad f(T) = \frac{n(0)}{n_1(T) + n(0)}\,, \tag{137}$$

$$n(0) = n_{\mathrm{d}} \exp\left(-\frac{e\varphi(0)}{T}\right) \left(1 - \frac{j}{\mu T n_{\mathrm{d}}} \int_{-L_1}^{0} \exp\frac{e\varphi(s)}{T}\,\mathrm{d}s\right),$$

$$n_1(T) = N_{\mathrm{e}}(T) \exp\left(-\frac{E_{\mathrm{D}}}{T}\right).$$

Here j is the density of the current across the barrier; μ is the electron mobility; $\varphi(x)$ is the distribution of the potential in the barrier zone; ε is the permittivity; f is the filling factor of a single dislocation — defined by one of the formulas in the set of expressions (137) on the basis of a variant of the theory of the current – voltage characteristics given in Ref. [53]; $N_{\mathrm{e}}(T)$ is the density of states in the conduction band; E_{D} is the position of the dislocation level relative to the bottom of the conduction band; $n(0)$ is the concentration of electrons at the barrier crest.

The relative capacitance of the barrier is given by the expression

$$C_{\mathrm{b}} = 7.8\,\frac{L_1(0) + L_2(0)}{L_1(V) + L_2(V)}\,, \tag{138}$$

where $L_{1,2}$ follows from a formula in the set of expressions (137).

The dependence of f on the dimensionless voltage $U = eV/T$ [Eqn (136)] is plotted in Fig. 18. The parameters used in the calculations were the same as in the experiments reported in Ref. [45]: $n_{\mathrm{d}} = 10^{14}\ \mathrm{cm}^{-3}$, $\varepsilon = 12$, and N_{e} are the density of the electron states in silicon. The procedure for determination of E_{D} is explained in the caption of the figure. The dependence $j(V)$ at temperatures $T = 264$ K and $T = 296$ K is plotted employing the coordinates used in Ref. [45]. Curves *1 – 4* correspond to different values of E_{D}. Curve *2* agrees best with the experimental results [45] if the experimental points are first shifted by one order of magnitude along the abscissa. As pointed out above, this shift is of parasitic origin (no other explanation is offered).

The arbitrary nature of the shift in Fig. 1 of Ref. [45] becomes obvious in particular when the capacitance – voltage characteristic given in Ref. [45] is analysed. Here, introduction of a similar renormalisation of V results in a qualitative disagreement between the theoretical and experimental values of the capacitance. Therefore, a comparison of the calculated dependence $C_{\mathrm{b}}(V)$ of expres-

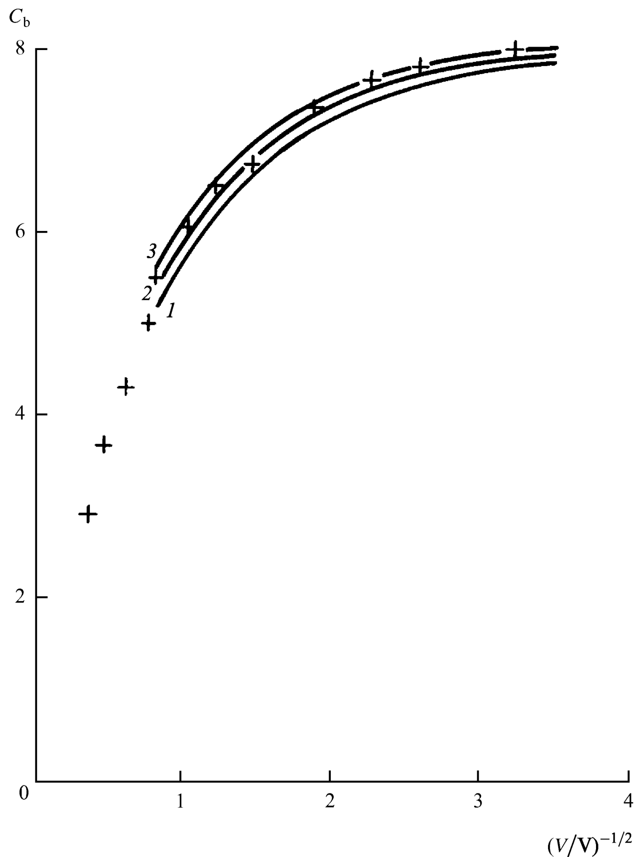

Figure 19. Comparison of the calculated capacitance–voltage characteristic $C_b(V)$ and the data of [45] without any correction. The value of C_b is plotted along the ordinate on the assumption that the theory and experiment (+) agree in the limit $V \to 0$. Curve 2 is closest to the experimental data; (1) $E_D = 0.65$ eV; (2) $E_D = 0.7$ eV; (3) $E_D = 0.75$ eV.

sion (138) and the results of Ref. [47] is made in Fig. 19 without any correction but employing the coordinates used in Ref. [45]. The dependence is fixed relative to the C_b axis on the assumption that the theory and experiment agree for $V \to 0$. According to Fig. 19, curve 2 with $E_D = 0.7$ eV is closest to the experimental results.

It therefore follows that the current–voltage and capacitance–voltage characteristics of a barrier given in Ref. [45] do indeed yield the different values of E_D and their ratio represents the extent to which the barrier in question can be regarded as one-dimensional. It follows from the ideas put forward above that $\gamma = 0.6/0.7 = 0.86$, i.e. the barrier is largely one-dimensional although the presence of saddle points at its crest is felt.

4.4.2 One of the problems in the interpretation of the current–voltage characteristics of barriers of different origin in semiconductors (such as those associated with grain boundaries, boundaries in bicrystals, dislocations, etc.) is the multivalued behaviour of the current–voltage characteristic in the intermediate range of the potential difference V between the barrier edges. In some cases [45] this characteristic has a plateau between the ohmic and nonlinear dependences of j on V (Fig. 18). In other experiments [55] such a plateau is not observed.

A qualitative explanation of this plateau (Fig. 18) can be found in a number of papers in which the one-dimensional model of a barrier with deep electron states localised at its crest is employed (see, for example, Refs [52–54]). An increase in the current across the barrier is in this case accompanied by an increase in the concentration of free electrons at the barrier crest and this, in turn, increases the occupancy factor of localised electron states at the crest and, consequently, increases the barrier height.

Barriers with saddle points may have no such plateau. Specific arguments in support of a monotonic nonlinearity of $j(V)$, i.e. in support of a current–voltage characteristic with $\partial j/\partial V > 0$, are given in Ref. [56] for a barrier that forms because of an overlap of the adjacent Read cylinders of a system of parallel charged dislocations distributed equidistantly with a period d, for example along the boundary of a bicrystal containing the y axis.

Let us assume that the degree of overlap h of the adjacent Read cylinders is small so that the chord b in Fig. 17 is much smaller than the radius of a Read cylinder R: $b \ll R$. Let us also assume that the radius R is much greater than the Debye radius r_D for a given n-type semiconductor $r_D^2 = \varepsilon T/(4\pi e^2 n_d)$, where ε is the permittivity of the semiconductor, n_d is the donor concentration, and T is the absolute temperature sufficiently high to assume that all the donor states are ionised, but still low compared with the barrier height $e\varphi_s$ at the saddle point. In the vicinity of an extremum of φ_s the potential $\varphi(x, y)$ is given by expressions (120)–(122):

$$e\varphi(x, y) = e\varphi_s + 0.5ky^2 - 0.5qx^2 + \ldots ,$$

$$\varphi_s = 4\pi e^2 n_d \varepsilon^{-1} h^2 , \quad k = 8\pi e^2 n_d \varepsilon^{-1} , \quad q = 8\pi e^2 n_d h \varepsilon^{-1} R^{-1} , \tag{139}$$

$$R \gg b \gg h \gg r_D , \quad T \ll e\varphi_s , \quad b \approx (2Rh)^{1/2} .$$

Here, k and q are the curvatures of the potential at a saddle point.

Under the conditions described by the set of expressions (139) the general problem of calculation of the current across a barrier can be divided into two parts. First, we have to determine the potential $\psi(r, \vartheta)$ across a barrier in the absence of a current through the barrier, and then we have to solve equation $\operatorname{div} \boldsymbol{j} = 0$ with a given distribution of the potential $\psi(r, \vartheta)$, proportional to the applied potential difference V.

Bearing in mind that $R \gg r_D$, we can formulate the task of finding the structure of $\psi(r, \vartheta)$ as the boundary-value problem:

$$\Delta\psi = 0 , \quad \psi(r, \vartheta)\Big|_{r=R} = \begin{cases} +V , & 0 \leqslant \vartheta \leqslant \pi - \alpha , \\ -V , & \pi + \alpha \leqslant \vartheta \leqslant 2\pi - \alpha , \end{cases} \quad \alpha = \frac{b}{R} \ll 1 . \tag{140}$$

The result is [compare with expression (128)]

$$\psi(r, \vartheta) = \frac{2V}{\pi} \arctan \frac{2Rr \sin(\vartheta)}{R^2 - r^2} . \tag{141}$$

The density of the additional surface charge along the boundaries of the Read cylinders is

$$\sigma(\vartheta) = \frac{\varepsilon}{4\pi} \frac{\partial\psi}{\partial r}\Big|_{r=R} = -\frac{\varepsilon V}{2\pi^2 R \sin(\vartheta)} , \quad |\vartheta| \geqslant \alpha . \tag{142}$$

The appearance of the charges $\sigma(\vartheta)$ in the above expression under the action of the potential difference V means that in reality the barrier boundaries shift relative to their

equilibrium positions in the absence of V by an amount $\xi(\vartheta)$:

$$\xi(\vartheta) = \frac{\sigma(\vartheta)}{en_{\mathrm{d}}}, \quad \xi_{\max} \ll b . \tag{143}$$

As a result, the barrier loses its symmetry relative to the plane containing charged dislocations. This is the main reason why in the one-dimensional model the appearance of a potential difference V at the barrier edges directly alters the conditions of occupation of the localised states at the barrier crest. In the case when $\xi(\vartheta)$ is described by expression (143) the shifts of the Read boundaries are very inhomogeneous. They are largest in the contact zones and small, in view of $b/R \ll 1$, far from these zones. Consequently, we can assume that in the zeroth approximation, in respect of the parameter $b/R \ll 1$, the origin of the coordinates of the problem described by expression (140) coincides with the position of a charged dislocation and there are no reasons why there should be a change in the density of free electrons in the Read cylinder axes under the influence of the potential difference V, because the potential $\psi(r, \vartheta)$ given by expression (141) vanishes in the limit $r \to 0$.

The current flowing across the barrier $e\varphi(x, y)$ is calculated in the diffusion approximation, i.e. it is assumed that

$$\operatorname{div} \mathbf{j} = 0 , \quad \mathbf{j} = -\mu\big[T\nabla n + en\nabla(\varphi + \psi)\big] \tag{144}$$

subject to the boundary conditions that correspond to the potential difference V at the barrier edges; here, μ is the electron mobility. Formally, the problem described by Eqn (144) is identical with the analogous problem of decay of a metastable state in the theory of first-order phase transitions, investigated in detail by Langer [48] [see also expressions (106) and (131)]. Omitting the relevant details of the calculation, we shall now give the final results for the dependence of the average density $\langle j_x \rangle$ of the current flowing through a given saddle point on the potential difference V:

$$\langle j_x \rangle = \langle j_x^0 \rangle \left(\frac{1 + 0.5eV}{T} + \ldots \right) ,$$

$$\langle j_x^0 \rangle = e\mu n_{\mathrm{d}} V d^{-1} \left(\frac{q}{k} \right)^{0.5} \exp(-e\varphi_{\mathrm{s}} T^{-1}) , \tag{145}$$

$$d = R - h , \quad h \ll R , \quad \xi_{\max} = b .$$

Obviously, the current – voltage characteristic described by expression (145) has no plateau.

4.4.3 The experiments reported in Ref. [46] deserve special consideration. First, these are the only experiments known to us which demonstrate explicitly the possibility of the existence of a 'neutral' component in the structure of dislocation barriers. In fact, the distribution of the etch pits revealed in these experiments (Fig. 20) is completely isotropic in the xy plane of the figure. However, the neutral wakes following each of the dislocations make the conductivity of the sample anisotropic along the x and y directions, as shown in Fig. 21. We are thus faced with an interesting problem of the properties of the current – voltage characteristic of a combined barrier with charged and neutral components. A description of such barriers is still lacking.

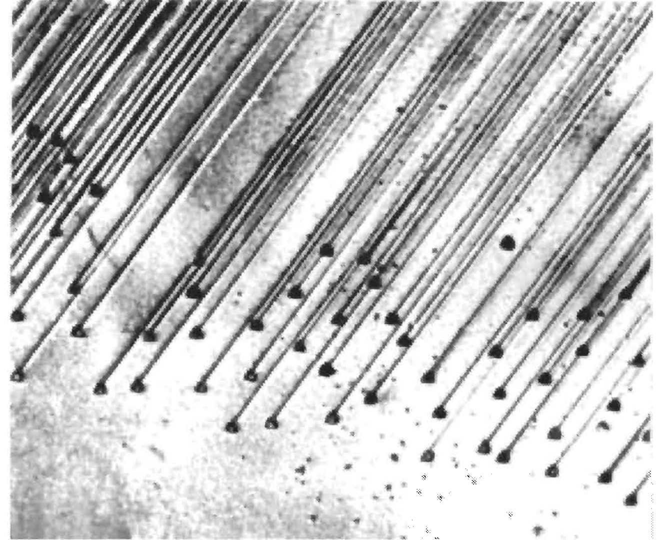

Figure 20. Effects of selective chemical etching of the surface of silicon, showing etch pits at dislocations and 'wakes' along glide planes.

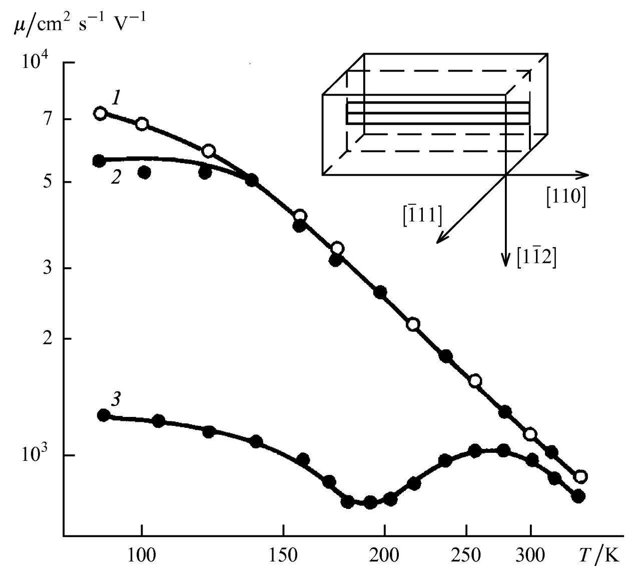

Figure 21. Temperature dependence of the electron mobility in plastically deformed silicon. The lines of flow of the current are directed perpendicular (*3*) to the glide plane and parallel to this plane (*1* and *2* along and across dislocations, respectively). The top part of the figure shows schematically a sample and the positions of dislocations and of the active glide plane [46].

Second, there is an interesting nonmonotonic temperature dependence of $\mu_{\perp}$, whereas the component $\mu_{\|}$ has no such minimum (Fig. 21). This nonmonotonic behaviour can be explained as follows. Immediately after the appearance of a 'fork' (i.e. of a difference between $\mu_{\|}$ and $\mu_{\perp}$) at about $T \approx 300$ K, the degree of anisotropy begins to rise and this corresponds to an increasing overlap of the adjacent Read cylinders. However, at $T \approx 200$ K, when the parameter $T = e^2 f/(\varepsilon a T)$ becomes comparable with unity, the barrier transparency begins to rise. This rise can be compared with the steep rise of the concentration of holes [see expression (12)], which results in an effective reduction of the negative nature of charged dislocations. An estimate of the

parameter Γ for silicon with $\varepsilon \approx 10$, $a \approx 5 \times 10^{-8}$ cm, and $f \approx 0.1$ shows that Γ passes through $\Gamma \approx 1$ in the vicinity of $T \approx 200$ K. It is natural to mention here the formally analogous behaviour of $\sigma_{\perp}$ in the experiments on n-type germanium [24] (see Fig. 9). However, the reasons for the nonmonotonic temperature dependence in the latter case are different. There is a change in the screening mechanisms, which occurs when free electrons are frozen out in n-type samples. It is the region of such a change that corresponds to the position of the minimum of $\sigma_{\perp}(T)$ in Fig. 9, as can be confirmed by examining the temperature dependence of the conductivity of a control sample and the behaviour of $\sigma_{\parallel}(T)$. In the case of the dependence $\sigma_{\perp}(T)$, the screening radius at temperatures $T \approx T_{\min}$ is described by formulas (32)–(34) and, under the conditions of a partial freeze-out of electrons, is considerably greater than the Read radius. Under these conditions the overlap of the adjacent Read cylinders is maximal and the anisotropy tends to its maximum. However, at temperatures $T < T_{\min}$ the chemical potential begins to drop to its position between the bottom of the conduction band and the energy of point donors, towards the donor energy. Consequently, the screening radius begins to approach its Read value again, which considerably increases the dislocation barrier transparency.

4.5 Current – voltage characteristic of a single charged dislocation in a semiconductor

One of the elegant effects that demonstrate breakdown of the local neutrality in the vicinity of dislocation lines in silicon and germanium semiconductor crystals is the asymmetry of the current–voltage characteristic when the current flows from the dislocation axis to the periphery of a semiconductor and vice versa. Relevant experiments carried out on single dislocations in silicon [57] and germanium [58] crystals demonstrate a clear diode effect of dislocation origin.

A description of the diode effect for a single charged dislocation is given in Ref. [59] on the basis of the Debye approximation when $V_{\mathrm{C}} < T$, where V_{C} is the energy of an electron in the electrostatic field of a charged dislocation on the axis of this dislocation, and T is the absolute temperature. However, in the case of real dislocations with an edge component in silicon and germanium it is found that the opposite inequality $V_{\mathrm{C}} > T$ is obeyed in a wide range of temperatures. Under these conditions the current–voltage characteristic of a single dislocation must be calculated anew, which was done in Ref. [60].

Let us assume that a dislocation core coincides with the z axis of a cylindrical coordinate system and that the steady-state current density $\boldsymbol{j}(\boldsymbol{r})$ is directed radially, so that $\operatorname{div}\boldsymbol{j} = 0$ and

$$\boldsymbol{j}(\boldsymbol{r}) = \frac{j_0 r_0}{r} \,. \qquad (146)$$

Here, r_0 is the minimum distance at which the local diffusion definition of the current density is still valid:

$$\boldsymbol{j}(\boldsymbol{r}) = \mu n(\boldsymbol{r}) \nabla \zeta(\boldsymbol{r}) \,, \qquad (147)$$

where μ is the electron mobility; $\zeta(\boldsymbol{r})$, $n(\boldsymbol{r})$ are, respectively, the local values of the chemical potential and of the electron concentration in the bulk of the semiconductor. If we assume that the difference between the chemical potentials of an electron on the dislocation axis and far from this axis (i.e. at a distance $r \geqslant R$, where R is the Read radius which governs the screening radius of the electric field of the dislocation) is eV (V is the applied potential difference), we can rewrite the definitions given by expressions (146) and (147) as follows:

$$j_0 = \frac{\mu V}{r_0 \displaystyle\int_{r_0}^{R} \left[r n(\boldsymbol{r}) \right]^{-1} \mathrm{d}r} \,. \qquad (148)$$

The explicit form of $n(\boldsymbol{r})$ can be deduced from the structure of $\zeta(\boldsymbol{r})$ in the limit of the Boltzmann statistics for electrons in the bulk of an n-type semiconductor where the donor concentration is n_{d} and the diffusion coefficient is D:

$$\nabla \zeta = e \nabla \varphi + T n^{-1} \nabla n \,, \qquad \mu = e D T^{-1} \,. \qquad (149)$$

In this case it follows from expressions (146)–(148) that

$$n(\boldsymbol{r}) = \exp\left(-\frac{e\varphi(\boldsymbol{r})}{T}\right) \left\{ n_{\mathrm{d}} - \frac{j_0 r_0}{D} \int_r^R r^{-1} \exp\left[\frac{e\varphi(\boldsymbol{r})}{T}\right] \mathrm{d}r \right\} , \qquad (150)$$

where the potential φ can be described by [see expression (8)]

$$\varphi(\boldsymbol{r}) = \frac{2ef}{\varepsilon a} \left[\ln \frac{R^2}{r} - 0.5 \left(1 - \frac{r^2}{R} \right) \right] , \quad \pi R^2 n_{\mathrm{d}} = \frac{f}{a} \,. \qquad (151)$$

Here f is the dislocation filling factor; ε is the permittivity; the explicit expression for the Read cylinder radius R is valid if $R \gg r_{\mathrm{D}}$, which is assumed to be obeyed; $r_{\mathrm{D}}^2 = \varepsilon T / (4\pi e^2 n_{\mathrm{d}})$; a is the interatomic spacing.

The definitions given by expressions (148)–(151) relate the quantities j_0, V, and f. We can deduce the current–voltage characteristic, i.e. the relationship between j_0 and V, from these definitions if we also define f in terms of E_{D} and V. The simplified variant of this definition is

$$-E_{\mathrm{D}} + eV + V_{\mathrm{C}} = \zeta(R) \,, \qquad V_{\mathrm{C}} = e\varphi\left(\frac{a}{f}\right) , \qquad (152)$$

where E_{D} is the position of the dislocation level in the band gap of the semiconductor measured from the bottom of its conduction band; $\zeta(R) \equiv F$ is the position of the chemical potential far from a dislocation; $\varphi(r)$ is given by expression (151).

The system of definitions (148)–(152) may be simplified considerably if we use the integral $\int [r n(\boldsymbol{r})]^{-1} \, \mathrm{d}r$ which occurs in the definition of j_0 given by expression (148). We consequently have

$$j_0 = \frac{D n_{\mathrm{d}}}{r_0} \, \frac{1 - \exp(-eV/T)}{\displaystyle\int_{r_0}^{R} r^{-1} \exp\big(e\varphi(r)/T\big) \, \mathrm{d}r} \,. \qquad (153)$$

This definition of j_0 resembles the familiar expression for the current–voltage characteristic obtained in the diffusion theory of rectification [61], which is not surprising since a charged dislocation can be regarded as a cylindrically symmetric Schottky barrier. The difference between these two expressions is only the presence of a truncating factor r_0, which can be regarded as the radius of a point which brings the current to the axis of a charged dislocation and the radius representing the capture of electrons by a dislocation level.

In the ohmic region and with logarithmic precision in terms of the parameter $R/r_0 \gg 1$, expression (153) can be reduced to

$$j_0 = \frac{Dn_{\rm d}}{r_0}\,\frac{eV}{T}\,2\Gamma\left(\frac{r_0}{R}\right)^{2\Gamma}, \quad \Gamma = \frac{e^2 f}{\varepsilon a T}\,. \tag{154}$$

A comparison of this expression with the experimental current–voltage characteristic of silicon [57] makes it possible to estimate r_0 for given values of $n_{\rm d} \approx 10^{14}$ cm^{-3} and $f \approx 0.1$ on the assumption that $T = 250$ K, $R \approx 10^{-4}$ cm, $\varepsilon \approx 12$, and $\rho = 150\ \Omega$ cm. The result is $2\Gamma(250\ {\rm K}) \approx 2$ and $r_0/R \approx 10^{-1}$. The same estimate of r_0/R can be obtained on the assumption that the slope of the current–voltage characteristic in the ohmic region, taken from Ref. [57], is approximately 30–50 times less than the slope of the characteristic of dislocation-free silicon (Fig. 22). Therefore, $2\Gamma(r_0/R)^{2\Gamma} \approx 1/50$ and hence for $\Gamma \approx 1$ we have $r_0/R \approx 10^{-1}$.

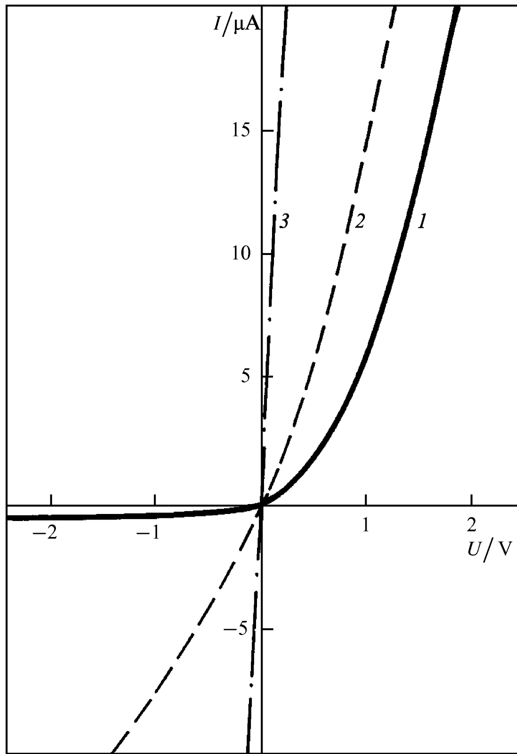

Figure 22. General appearance of the current–voltage characteristic of a single dislocation obtained with: (1) a microprobe located at a point of emergence of a 60° dislocation; (2) a microprobe located above a dislocation-free surface; (3) two gold ohmic contacts [57].

5. Relaxation phenomena

The problem of establishment of an equilibrium in the electron system of a semiconductor containing charged disloca-tions is in a surprisingly uncertain state. On the one hand, there are no doubts about the qualitative features of the relaxation phenomena which occur in plastically deformed semiconductors, for example, the nonexponen-tial (logarithmic) time dependence of the nonequilibrium photocon-ductivity after its significant (nonlinear) devia-tion from the equilibrium value [62]. On the other hand, there are absolutely no published quantitative details on even the simplest relaxation effect represented by the exponential relaxation asymptote typical of the linear stage of various relaxation processes. The neglect of this problem is particularly striking against the background of the success of the experimental and theoretical studies of the relaxation involving point centres (see, for example, Ref. [63]).

Experimentalists are obviously put off by the routine nature of the problem of the exponential relaxation processes. The existence of such relaxation is not in doubt and interpretation of the experimental relaxation time, particularly of the pre-exponential factor which governs the capture cross section, is very difficult. We are aware of only one fairly detailed investigation of the relaxation of the photoconductivity in germanium with a low dislocation density, when the adjacent Read cylinders do not overlap [62]. The traditional analysis of the results reported in Ref. [62], carried out below, gives an unexpected result: at low temperatures the electron capture cross section of a dislocation is anomalously large (it exceeds the dimensions of a sample!), which cannot be true. A discussion of possible reasons for this paradox leads to an interesting alternative for the description of the relaxation phenomena involving dislocations.

5.1 Exponential relaxation

5.1.1 We shall use the term 'traditional formalism' for the approach in which relaxation of the filling factor f of a single charged dislocation in an n-type semiconductor is described by the following equation [11, 62]:

$$\dot{f} = 2\pi a r_0 v_{\rm T}\left[\tilde{n}(1-f) - n_{\rm e} f\right], \quad \dot{f} \equiv \frac{{\rm d}f}{{\rm d}t}\,, \tag{155}$$

where

$$\tilde{n} = n_{\rm d}\exp\left(-\frac{V_{\rm C}}{T}\right), \quad V_{\rm C} \approx \frac{2e^2 f}{\varepsilon a}\ln\frac{R}{c}\,,$$

$$c = \frac{a}{f}\,, \quad \pi R^2 n_{\rm d} = \frac{f}{a}\,,$$

$$n_{\rm e} = N_{\rm e}\exp(-E_{\rm d}T^{-1})\,, \quad f < 1\,.$$

Here, $n_{\rm e} = n_{\rm d}$ is the electron concentration far from a dislocation (it is assumed that all the donors whose concentration is $n_{\rm d}$ are ionised); R is the Read radius; ε is the permittivity of the semiconductor; $E_{\rm d}$ is the depth of a dislocation level measured from the bottom of the conduction band; $v_{\rm T}$ is the thermal velocity of electrons; a is the atomic spacing along a dislocation; r_0 is the dislocation-capture length; $\tilde{n}$ is the local concentration of electrons on the dislocation axis; T is the absolute temperature; $N_{\rm e}$ is the density of the electron states in the conduction band.

If the equilibrium value f_0 is only slightly perturbed so that

$$f(t) = f_0 + \delta f(t)\,, \quad \delta f \ll f_0\,, \tag{156}$$

Eqn (155) is linearised and, with a logarithmic precision [on the assumption that $\ln(R/c) \gg 1$], it becomes

$$\delta\dot{f} = -\frac{\delta f}{\tau_0}\,, \quad \tau_0^{-1} = 2\pi a r_0 v_{\rm T}\, n_{\rm e}\,\frac{2e^2 f_0}{\varepsilon a T}\ln\frac{R_0}{c_0}\,, \tag{157}$$

where

$$\pi R_0^2 n_{\rm d} = \frac{f_0}{a}\,, \quad c_0 = \frac{a}{f_0}\,,$$

and τ_0 is the characteristic relaxation time. The quantity r_0, calculated with the aid of Eqn (157) and the experimental data [62] on the photoconductivity relaxation time τ_0 of n-type germanium containing charged dislocations, is presented in Table 1 [64] where other relevant quantities are also given. The value of r_0 varies in the range $10^3 \geqslant r_0 \geqslant 10^{-8}$ cm. Obviously, the amplitude of this change is too large to correspond to any physical meaning of r_0 in Eqn (157).

Table 1.

T/K	f	R/cm	2τ	τ^*/s	r_0/cm	r_σ/cm
80	0.13	2.9×10^{-4}	6.25	10^3	10^2	10^{-6}
100	0.12	2.8×10^{-4}	5	50	0.83	5×10^{-7}
125	0.11	2.64×10^{-4}	4.0	10	3×10^{-5}	1.4×10^{-7}
170	0.09	2.4×10^{-4}	2.94	6×10^{-1}	2×10^{-8}	0.7×10^{-7}
200	0.08	2.25×10^{-4}	2.5	8×10^{-3}	1×10^{-8}	0.4×10^{-7}

Note. The results were obtained for weakly deformed n-type germanium with the following parameters: $\varepsilon = 16$, $E_D = 0.4$ eV below the conduction band, $a = 5\times10^{-8}$ cm, $n_d = 5\times10^{13}$ cm^{-3}, and $\sigma = 0.5\times10^{11}$ s^{-1}. The value of r_0 was calculated on the assumption that $\tau^* = \tau_0$, with τ^* taken from this table and τ_0 from expression (157); the value of r_σ was obtained on the assumption that $\tau^* = \tau_\sigma$, where τ_σ is given by expression (166). The data for $T = 80$ K were taken from Ref. [23] and the rest of the information on T, f, and τ^* was obtained from Ref. [62].

5.1.2 It is assumed in Eqn (157) that the main obstacle preventing a bulk electron from reaching a dislocation is the transition from the continuous spectrum to a discrete level. The probability of this transition is proportional to the capture length r_0. However, in reality there is one other reason that hinders the transition of electrons from the bulk to a dislocation level. This reason is the conductivity σ of a Read cylinder. If we assume that the main reason for the finite relaxation time is the finite conductivity of the semiconductor, we can write down a new relaxation equation which is an alternative to Eqn (157); we can then use this new equation to find the corresponding relaxation time τ_σ.

An alternative equation can be obtained on the basis of the following assumptions and simplifications.

The electron current in the interior of a Read cylinder can be described in terms of a local (diffusion) approximation:

$$j(r) = \frac{\mu}{e}\, n(r)\nabla\zeta\ . \tag{158}$$

Here, μ is the electron mobility; $\zeta(r)$ and $n(r)$ are the local values of the chemical potential and of the electron concentration. The definition of $j(r)$ given by expression (158) is valid up to the minimum distance r_σ, beyond which in the range $r < r_\sigma$ the diffusion approximation of expression (158) becomes invalid. However, in this range an electron may be captured by a dislocation level. The length r_σ thus plays the role of the capture length r_0, which occurs in expressions (155) and (157). The value of r_σ is not calculated and it remains a parameter of the theory.

In the vicinity of $r \approx r_\sigma$ the local values of the bulk chemical potential $\zeta(r)$ and of the chemical potential ζ_D of electrons on a dislocation are equal:

$$\zeta(r_\sigma) = \zeta_D\,, \quad \zeta_D = -E_D + V_C\ . \tag{159}$$

Here, the definitions of E_D and V_C are analogous to those given following Eqn (155). The requirements defined by expression (159) mean that an electron which has 'lifted itself' to the region $r \approx r_\sigma$ can penetrate without difficulty to a dislocation level. In writing down the chemical potential ζ_D of the dislocation electrons, we ignored, for the sake of simplicity, the entropy contribution because both E_D and V_C are much greater than the corresponding energy equivalent of temperature.

We shall simplify the analysis by postulating that the problem is cylindrically symmetric, which is generally incorrect because at short distances $r = r_\sigma$ a considerable contribution to the relaxation displacements of the bulk electrons is made by the anisotropic deformation potential.

The initial relaxation equation is now

$$\dot{f} = -2\pi a r_\sigma j_\sigma\ , \tag{160}$$

where j_σ is the bulk flux of electrons at the distance $r = r_\sigma$ from the cylinder axis. If we assume that the characteristic time needed to establish an electron flux in a Read cylinder is much shorter than the dislocation relaxation time

$$\tau_\sigma \gg \tau_D\ , \quad \tau_D \approx \frac{R^2}{D}\ , \quad \mu = \frac{eD}{T} \tag{161}$$

[the above inequality is justified after the definition of the time τ_σ given by formula (166)], we can assume that the electron current density $j(r)$ satisfies the requirement $\operatorname{div}\mathbf{j} = 0$, i.e.

$$j(r) = j_\sigma r_\sigma r^{-1}\ , \quad r \geqslant r_\sigma\ . \tag{162}$$

The definition (158) and the boundary conditions (159) lead to the following expression for j_σ, which is deduced from Eqn (160):

$$j_\sigma = -\frac{\mu}{e r_\sigma}\,\frac{\zeta_\infty + \zeta_D - V_C}{\displaystyle\int_{r_\sigma}^{R} \mathrm{d}r/rn(r)}\ , \quad V_C = e\varphi(c)\ , \tag{163}$$

$$e\varphi(r) = \frac{2e^2 f}{\varepsilon a}\left[\ln\frac{R}{r} - 0.5\,(1 - r^2R^{-2})\right]\ , \tag{163a}$$

$$(r) = \exp\left(-\frac{e\varphi}{T}\right)\left(n_d - \frac{j_\sigma r_\sigma}{D}\int_r^R \frac{\mathrm{d}r}{r}\exp\frac{e\varphi}{T}\right)\ , \tag{163b}$$

where ζ_∞ is the chemical potential measured from the bottom of the conduction band, outside the Read cylinder.

Obviously, under equilibrium conditions and with logarithmic precision we have

$$\zeta_\infty + E_D - V_C = 0\ . \tag{164}$$

This requirement is the definition of the equilibrium occupation factor f_0. However, if the combination in expression (164) differs from zero, the current j_σ of expression (163) appears and, according to Eqn (160), the value of f may vary with time.

The integral which occurs in the definition of j_σ by expression (163) can be calculated. As a result, Eqn (160) subject to expression (163) becomes

$$j = 2\pi\Gamma\sigma\left(\frac{r_\sigma}{R}\right)^{2\Gamma}\left(1 - \exp\frac{\delta\zeta}{T}\right)\ , \tag{165}$$

where

$$\delta\zeta = \zeta_\infty + E_D - V_C\ , \quad \sigma = \frac{n_d e^2\tau}{m^*}\ , \quad \mu = \frac{eD}{T} = \frac{e\tau}{m^*}\ .$$

Here, τ is the momentum relaxation time for electrons scattered by the lattice defects; σ is the conductivity in the τ approximation; m^* is the effective mass of an electron; Γ and V_C are defined by expressions (154) and (155).

Linearisation of expression (165) in the range $\delta\zeta < T$ gives the definition of τ_σ which represents the relaxation time of charged dislocations due to the finite conductivity σ [64]:

$$\tau_\sigma^{-1} = \frac{2\pi\sigma}{\varepsilon\Gamma_*} \ln \frac{R_0^2}{c_0^2}, \quad \Gamma_* = \frac{1}{\Gamma}\left(\frac{R_0}{r_\sigma}\right)^{2\Gamma} \gg 1 . \tag{166}$$

An analysis of the results of Ref. [64] (together with the information on τ_σ at $T = 80$ K taken from Ref. [23]) and the use of τ_σ defined by the above expression gives values of r_σ listed in Table 1. The range of variation of r_σ with temperature T is $10^{-7} \leqslant r_\sigma < 10^{-6}$ cm, which looks more reasonable than the range of variation of r_0 which follows from expression (157).

We shall conclude by noting that the finite conductivity of a Read cylinder may be one of the important factors that influence the exponential relaxation time. In the experiments reported in Ref. [62] this relaxation channel is the dominant one.

A few words should be said about the physical factors that determine the capture radius r_0. Determination of the capture cross section is a difficult kinetic problem [63]. Nevertheless, in this case of dislocations there are clear energy considerations which make it possible to estimate qualitatively the capture radius [65].

This can be done because the combination of the Coulomb potential of expression (8) and of the deformation potential $V_\xi(r, \vartheta)$ around a charged dislocation is characterised by a saddle point r_0 through which electrons are most likely to penetrate from the bulk of a semiconductor to a dislocation. The position of this saddle point can be found from

$$\frac{\partial}{\partial r}\left[V_C(r) - V_\xi\left(r, \frac{\pi}{2}\right)\right] = 0 , \tag{167}$$

which finally gives

$$r_0 = \frac{(1-2\upsilon)}{2\pi(1-\upsilon)} \frac{W}{V_C^0} b, \quad V_C^0 = \frac{2e^2 f}{\varepsilon a} . \tag{168}$$

The scale r_0 for germanium is $r_0 \geqslant 10^{-6}$ cm.

5.2 Logarithmic relaxation

In discussing the relaxation phenomena involving charged dislocations we cannot ignore the logarithmic relaxation mechanism. This specific mechanism is observed only for linear charged defects and was discovered by Figielski and his colleagues [62] (Fig. 23). This is one of the nonlinear effects described by Eqn (155).

Let us assume that initially there is an abrupt change δf in the occupancy factor, which tends to reduce it. Recovery of the equilibrium then occurs mainly by inflow of electrons from the bulk of a semiconductor to a dislocation (the outgoing term is unimportant). If we additionally assume that

$$f = f_0 + \delta f, \quad \delta f < f_0, \quad \text{but} \quad \frac{2e^2\delta f}{\varepsilon a T} \gg 1 , \tag{169}$$

we find from Eqn (155) that

$$\delta\dot{f} = \tau_*^{-1} \exp(-\lambda\delta f) ,$$

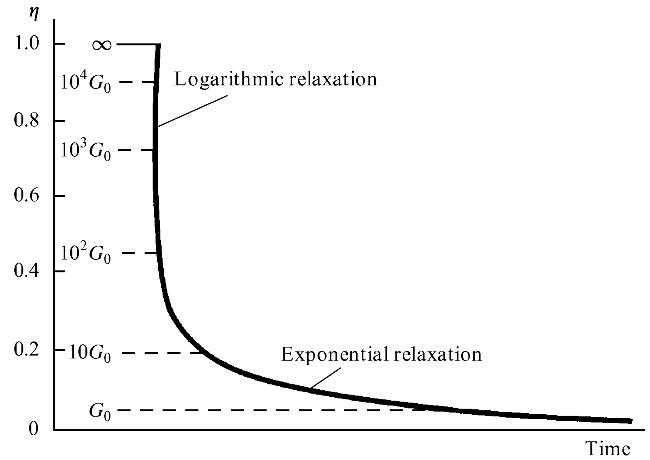

Figure 23. Low-temperature relaxation of the photocurrent in n-type germanium containing charged dislocations. The horizontal dashed lines represent different initial illumination intensities [62].

$$\tau_*^{-1} = \langle\sigma\upsilon\rangle\, n_\infty (1 - f_0) \exp\left(\frac{eV_C^0}{T}\right) , \tag{170}$$

$$\lambda = \frac{2e^2}{\varepsilon a T} \ln \frac{R_0}{c_0}$$

or

$$\exp(\lambda\delta f) - 1 = \frac{\lambda t}{\tau_*}, \quad \lambda\delta f = \ln\left(1 + \frac{\lambda t}{\tau_*}\right) . \tag{171}$$

Here, V_C^0 is given by expression (168).

The result, $\delta f \propto \ln t$ is specific to linear charged defects. At present, this property is used widely for the diagnostics of charged dislocations in the investigated crystals. It appears very effectively in DLTS experiments on charged dislocations (see, for example, Ref. [66]). However, a discussion of the details of the DLTS experiments is outside the scope of this review.

6. Conclusions

We shall conclude this review by pointing out once more that the majority of the experimental data on charged dislocations in germanium and silicon can be explained in a self-consistent manner by a system of levels shown in Fig. 5. This system is of phenomenological origin, i.e. it does not answer the question of the actual positions of levels in the band gap of a semiconductor or on the smallness of the capacities C_1 of the lower acceptor levels E_1. Nevertheless, the system is very useful.

Various spectroscopic methods for the investigation of dislocations in semiconductors are being developed rapidly. These methods can provide information on the role of the deformation potential, on the influence of splitting of dislocations, on the specific effects of point impurities localised near the cores of charged dislocations, etc. These topics require a separate review.

Acknowledgements. We are deeply grateful to Yu A Osip'yan and W Schroter for their interest and numerous stimulating discussions of the physics of charged dislocations in semiconductor crystals.

References

1. Gallagher C J *Phys. Rev.* **88** 721 (1952)
2. Shockley W *Phys. Rev.* **91** 228 (1953) [abstract]
3. Read W T Jr *Philos. Mag.* **45** 775 (1954)
4. Read W T Jr *Philos. Mag.* **45** 1119 (1954)
5. Pearson G L, Read W T Jr, Morin F L *Phys. Rev.* **93** 666 (1954)
6. Logan R A, Pearson G L, Kleinman D A *J. Appl. Phys.* **30** 885 (1959)
7. Labusch R, Schroter W, in *Dislocations in Solids* (Ed. F R N Nabarro) Vol. 5 *Other Effects of Dislocations. Disclinations* (Amsterdam: North-Holland, 1980) Chap. 20, pp 127 – 192
8. Ossipyan Yu A *Sov. Sci. Rev. A* **4** 219 (1982)
9. Matare H F *J. Appl. Phys.* **56** 2605 (1984)
10. Ossipyan Yu A, Petrenko V F, Zaretskii A V *Adv. Phys.* **35** 115 (1986)
11. Bonch-Bruevich V L, Kalashnikov S T *Fizika Poluprovodnikov* (Physics of Semiconductors) (Moscow: Nauka, 1977)
12. Bonch-Bruevich V L, Glasko V B *Fiz. Tverd. Tela (Leningrad)* **3** 39 (1961) [*Sov. Phys. Solid State* **3** 26 (1961)]
13. Kveder V V, Kravchenko V Ya, Mchedlidze T R, et al. *Pis'ma Zh. Eksp. Teor. Fiz.* **43** 202 (1986) [*JETP Lett.* **43** 255 (1986)]
14. Kveder V V, Mchedlidze T R, Osip'yan Yu A, Shalynin A I *Zh. Eksp. Teor. Fiz.* **93** 1470 (1987) [*Sov. Phys JETP* **66** 838 (1987)]
15. Kveder V V, Mchedlidze T R, Osip'yan Yu A, Shalynin A I *Fiz. Tverd. Tela (Leningrad)* **32** 2224 (1990) [*Sov. Phys. Solid State* **32** 1292 (1990)]
16. Landauer R W *Phys. Rev.* **94** 1386 (1954)
17. Bonch-Bruevich V L *Fiz. Tverd. Tela (Leningrad)* **3** 47 (1961) [*Sov. Phys. Solid State* **3** 34 (1961)]
18. Emtage P R *Phys. Rev.* **163** 865 (1967)
19. Claesson A *Phys. Status Solidi B* **61** 599 (1974)
20. Winter S *Phys. Status Solidi B* **79** 637 (1977)
21. Nabutovskii V M, Shapiro B Ya *Zh. Eksp. Teor. Fiz.* **75** 948 (1978) [*Sov. Phys. JETP* **48** 480 (1978)]
22. Voronov V P, Kosevich A M *Fiz. Nizk. Temp.* **6** 371 (1980) [*Sov. J. Low Temp.* **6** 177 (1980)]
23. Kolyubakin A I, Osip'yan Yu A, Shevchenko S A *Zh. Eksp. Teor. Fiz.* **77** 975 (1979) [*Sov. Phys. JETP* **50** 491 (1979)]
24. Kolyubakin A I, Shevchenko S A *Pis'ma Zh. Eksp. Teor. Fiz.* **30** 208 (1979) [*JETP Lett.* **30** 189 (1979)]
25. Schroter W *Phys. Status Solidi* **21** 211 (1967)
26. Osip'yan Yu A, Shevchenko S A *Zh. Eksp. Teor. Fiz.* **65** 698 (1973) [*Sov. Phys. JETP* **38** 345 (1974)]
27. Kolyubakin A I, Shevchenko S A *Phys. Status Solidi A* **63** 677 (1981)
28. Grazhulis V A, Kveder V V, Mukhina V Yu *Phys. Status Solidi A* **43** 407 (1977)
29. Kamke E *Differentialgleichungen, Losungsmethoden und Losungen* Vol. 1 *Gewohnliche Differentialgleichungen* (Leipzig: Akademische Verlagsgesellschaft, 1942; reprinted New York: Chelsea, 1971)
30. Glazman L I, Suris R A *Fiz. Tekh. Poluprovodn.* **20** 1769 (1986) [*Sov. Phys. Semicond.* **20** 1109 (1986)]
31. Shikin V B, Shikina Yu V *Fiz. Tekh. Poluprovodn.* **25** 2225 (1991) [*Sov. Phys. Semicond.* **25** 1341 (1991)]
32. Shikina Yu V, Shikin V B *Fiz. Tekh. Poluprovodn.* **26** 987 (1992) [*Sov. Phys. Semicond.* **26** 553 (1992)]
33. Bazhenov A, Shikina N, Shikina Yu *Fiz. Tverd. Tela (Leningrad)* **34** 789 (1992) [*Sov. Phys. Solid State* **34** 422 (1992)]
34. Vul B M, Zavaritskaya E I *Zh. Eksp. Teor. Fiz.* **76** 1089 (1979) [*Sov. Phys. JETP* **49** 551 (1979)]
35. Zavaritskaya E I *Pis'ma Zh. Eksp. Teor. Fiz.* **40** 116 (1984); **41** 231 (1985) [*JETP Lett.* **40** 864 (1984); **41** 279 (1985)]
36. Landwehr G, Handler P *J. Phys. Chem. Solids* **23** 891 (1962)
37. Gergel' V A, Suris R A *Fiz. Tekh. Poluprovodn.* **16** 1925 (1982) [*Sov. Phys. Semicond.* **16** 1243 (1982)]
38. Hirth J P, Lothe J *Theory of Dislocations* (New York: Wiley, 1968)
39. Bir G L, Pikus G E *Symmetry and Strain-Induced Effects in Semiconductors* (Jerusalem: Israel Program for Scientific Translations, 1975; New York: Wiley, 1975)
40. Baranskii P I, Kolomoets V V *Phys. Status Solidi B* **45** K55 (1971)
41. Shikina Yu V, Shikin V B *Fiz. Tekh. Poluprovodn.* **28** 675 (1994) [*Semiconductors* **28** 403 (1994)]
42. Eremenko V G, Nikitenko V I, Yakimov E B, Yarykin N A *Fiz. Tekh. Poluprovodn.* **12** 273 (1978) [*Sov. Phys. Semicond.* **12** 157 (1978)]
43. Koveshnikov S V, Feklisova O V, Yakimov E B, Yarykin N A *Phys. Status Solidi A* **127** 67 (1991)
44. Shikina Yu V, Shikina N I *Fiz. Tekh. Poluprovodn.* (in press)
45. Eremenko V G, Farber B Ya, Yakimov E B *Fiz. Tekh. Poluprovodn.* **17** 1313 (1983) [*Sov. Phys. Semicond.* **17** 831 (1983)]
46. Eremenko V G, Nikitenko V I, Yakimov E B *Pis'ma Zh. Eksp. Teor. Fiz.* **26** 72 (1977) [*JETP Lett.* **26** 65 (1977)]
47. Shklovski B I, Efros A L *Electronic Properties of Doped Semiconductors* (Berlin: Springer Verlag, 1984)
48. Langer J S *Ann. Phys. (New York)* **54** 258 (1969)
49. Veliev Z A, Shikina N I, Shikin V B *Fiz. Tekh. Poluprovodn.* **17** 153 (1983) [*Sov. Phys. Semicond.* **17** 97 (1983)]
50. Veliev Z A, Shikin V B *Fiz. Tekh. Poluprovodn.* **19** 858 (1985) [*Sov. Phys. Semicond.* **19** 528 (1985)]
51. Shikina Yu V, Shikin V B *Fiz. Tekh. Poluprovodn.* **26** 992 (1992) [*Sov. Phys. Semicond.* **26** 556 (1992)]
52. Taylor W E, Odell N H, Fan H Y *Phys. Rev.* **88** 867 (1952)
53. Gol'dman E I, Zhdan A G *Fiz. Tekh. Poluprovodn.* **10** 1839 (1976) [*Sov. Phys. Semicond.* **10** 1098 (1976)]
54. Gol'dman E I, Gulyaev I B, Zhdan A G, Sandomirskii V B *Fiz. Tekh. Poluprovodn.* **10** 2089 (1976) [*Sov. Phys. Semicond.* **10** 1244 (1976)]
55. McGonigal G C, Thomson D J, Shaw J G, Card H C *Phys. Rev. B* **28** 5908 (1983)
56. Shikina N I, Shikin V B *Fiz. Tekh. Poluprovodn.* **24** 749 (1990) [*Sov. Phys. Semicond.* **24** 471 (1990)]
57. Eremenko V G, Nikitenko V I, Yakimov E B *Zh. Eksp. Teor. Fiz.* **69** 990 (1975) [*Sov. Phys. JETP* **42** 503 (1975)]
58. Hess K J *Diplomarbeit* (Clausthal-Zellerfeld, Germany: University Press, 1989)
59. Vinokur V M, Kravchenko V Ya *Fiz. Tekh. Poluprovodn.* **9** 1346 (1975) [*Sov. Phys. Semicond.* **9** 887 (1975)]
60. Shikin V B, Shikina Yu V *Fiz. Tekh. Poluprovodn.* **25** 1065 (1991) [*Sov. Phys. Semicond.* **25** 642 (1991)]
61. Ansel'm A I *Introduction to Semiconductor Theory* (Moscow: Mir, 1981; Englewood Cliffs, NJ: Prentice-Hall, 1981)
62. Jastrzebska M, Figielski T *Phys. Status Solidi* **7** K101 (1964)
63. Abakumov V N, Perel' V I, Yassievich I N *Fiz. Tekh. Poluprovodn.* **12** 3 (1978) [*Sov. Phys. Semicond.* **12** 1 (1978)]
64. Shikina N I, Shikin V B *Fiz. Tekh. Poluprovodn.* **24** 749 (1990) [*Sov. Phys. Semicond.* **24** 471 (1990)]
65. Shikin V B, Shikina N I *Phys. Status Solidi A* **108** 699 (1988)
66. Kveder V V, Osipyan Yu A, Schroter W, Zoth G *Phys. Status Solidi A* **72** 701 (1982)